—Mini Review—

Human Sperm Processing in Assisted Reproduction Technology

Satoru Kaneko[1]

[1]Department of Obstetrics and Gynecology, Ichikawa General Hospital, Tokyo Dental College, 5-11-13 Sugano, Ichikawa, Chiba 272-8513, Japan

Abstract: *In ART, once ovum is successfully yielded, embryologists have to progress the treatments as arranged regardless of the quality of semen. Sperm qualities are, therefore, the most variable factor in each case. Embryologist is certainly well informed about physiology and genetics of ovum and embryo, it is also essential to study how to evaluate and prepare the sperm according to their physiology.*

Key words: *Human sperm, ART, DNA, Motility*

Progress in assisted reproduction technology (ART) has intended to make shortened the distance between the male and female gametes prior to fertilization. Intrauterine insemination (IUI) omits the passage through the cervix artificially, and IVF-ET facilitates the fertilization by incubating the oocyte and the sperm, *in vitro*. The ultimate method, intra-cytoplasmic sperm injection (ICSI), the distance between the two types of gametes becomes 0 by means of artificial injection. The aim of sperm preparation in ART is to deputize for some of the events which occur in the female genital tract.

Spermatogenesis

Sperm is the end product of the process of gametogenesis in the male, occurring within the seminiferous tubules of the testes. This involves a series of meiotic divisions of spermatogonial stem cells, two meiotic divisions by spermatocytes, extensive morphological remodeling of the spermatid during spermatogenesis, and the release of the free cell into the lumen of the seminiferous tubule by spermiation. It is an interesting paradox that the process of spermatogenesis produces a cell that is highly differentiated in structure and function, while at the same time is developmentally totipotent, being able to combine with an egg and thereby begin the process that give rise to a new individual.

Received: January 21, 2005
Accepted: February 7, 2005

Ejaculate

Many millions of sperm are produced daily in the testes, these are stored in the epididymis and released at regular intervals (ejaculation). The ejaculate once coagulates and liquefies at room temperature after about 10–30 min due to protein splitting enzymes from the prostate. Although the semen contains a variety of components, only the sperm with progressive motility start to penetrate into the cervical mucus and finally a small part of them reach the ampulla of the uterine tube. All the other components such as immotile sperm, bacteria, leucocytes, and the seminal plasma remain in the vagina.

Sperm DNA

Mammalian sperm has two main components, the head and tail. The head consists of the acrosome, the nucleus and a small amount of cyto-skeltal structures and cytoplasm. The acrosome is a large secretory granule that closely surrounds and overlies the anterior end of the nucleus. The sperm nucleus is haploid, containing only one member of each chromosome pair, and chromatin becomes highly condensed during the latter part of spermatogenesis. The volume of the sperm nucleus is less than that of somatic cells, and its chromatin is highly condensed. The sperm nucleus is unique, both in the amount of DNA present and in the composition of its nucleoproteins. The major nucleoproteins associated with sperm DNA are protamines. These are relatively small (27–65 amino acids) highly basic proteins rich in arginine and cysteine. The highly condensed DNA-protamine

complex is stabilized by disulfide bonds between protamines.

Programmed cell death is recognized as an essential event in morphogensis as well as normal turnover of cells [1], and it is known as apoptosis, which distinguishes it from necrosis or pathologic cell death [2]. Apoptosis plays important roles in germ cell loss [3]. It is the dominant process during spermatogenesis and is regulated by p53, p21, caspase, bcl2, and Fas expression levels, with many alternative path ways [4]. It is commonly recognized that human ejaculate contains heterogeneous sperm populations, which possess a variety of abnormalities at nuclear, cytoskeletal and organelle levels. To date, numerous authors have reported the existence of sperm with DNA damage, and the rate was increased in severe oligo-asthenozoospermia [5, 6].

Quality assurance of human sperm provided for ICSI

Since ICSI has diminished the quantitative limitation of sperm required for insemination as minimum as possible, it is accepted that most male infertilities can be overcome, except azoospermia. In ICSI, the injection of sperm is regarded as the transplantation of male chromosomes into the oocyte. As described above, the ejaculate has a heterogeneous sperm population. The selection of sperm in ICSI is, however, merely based on motility and gross morphology under a low magnification microscope. There is no proven method for sorting sperm by DNA integrity. The quality assurance of the sperm for the injection, especially the integrity of the DNA structure, is a minimum premise for the clinical application of ICSI in severe male infertility.

To resolve the above issue, three innovative technologies are necessary. First, we need to develop some methods to measure nuclear damage at multiple levels such as chromosome, gene and DNA structures in individual human sperm with high detection sensitivity. Second, the sperm, which possess DNA damage prior to ejaculation, have to be eliminated by means of the *in vitro* processing, and post-ejaculate DNA degradations have to bereduced to the minimum.

Significance of human sperm preparation in ART

During migration in the female genital tract, the sperm is selected and undergoes various physiological changes to achieve fertilization. The aim of sperm selection in ART is to synthesize these events by the *in vitro* processing. The ejaculate is polluted with bacteria during passage through the urethral orifice. Bacteria should be sterilized by the addition of antibiotics to the suspension or separated physically according to the differences in their apparent densities. After centrifugation, the sediment (sperm) is often recovered by aspirating the supernatant with a Pasteur pipette. In this way, a part of the supernatant adhering to inner surface of the tube descends, and the sediment is re-polluted with bacteria.

The ejaculate includes not only the sperm but also a variety of debris such as fine urethral calculus, mucinous gel, fibers of under wear, etc. Bacterial colonies are often observed on the surface of debris. The density gradient centrifugation technique is capable of separating free bacteria in the ejaculate, whereas those adhering to the debris are recovered in the sediment. After liquefaction, a small number of sperm with progressive motility start to penetrate into the cervical mucus, and all other components remain in the vagina.

To date, various procedures for sperm preparation have been reported [7–10]. Figures 1 and 2 show sperm preparation procedure to exclude debris in the ejaculate and for selecting the sperm with progressive motility. Prior to centrifugation, the debris has to be excluded by means of unit gravity sedimentation and subsequent filtration (ART filter, Nipro, Japan). The resulting suspension is condensed by the cushion method. Then the concentrated fraction is loaded on 5.0 ml of 90% Percoll in a separable fine neck tube (SFNT, Nipro, Japan), which is squeezed at the bottom to make the volume of sediment as small as possible. The linear density gradient is created by slow rotation, and centrifuged at 400x g for 30 min. To recover the sperm precipitated in the bottom of the tube, the top of the tube is plugged with a rubber cap, and the middle of the squeezed bottom is snapped off to avoid recontamination of the sediment by the seminal plasma and bacteria.

The motile sperm are separated by the modified swim-up method. The motile sperm are allowed to swim-up at 37°C, and the upper layer containing swum-up sperm is collected.

Observation of DNA fragmentation in human sperm

To observe DNA fragmentation in individual sperm, we employ single cell gel electrophoresis. The sperm is

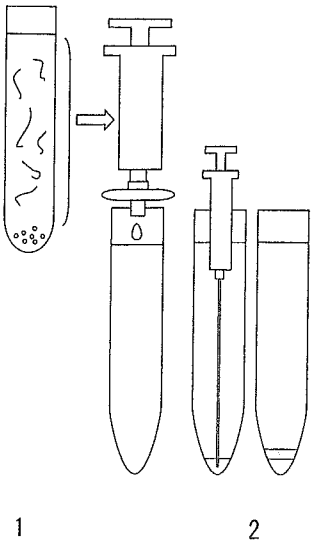

Fig. 1. Semen pretreatment prior to centrifugation. 1. Dilute semen and allow to precipitate debris. 2. Filtrate the suspension, introduce 0.1 ml Percoll to the bottom of the tube, then centrifuge (cushion method), then centrifuge.

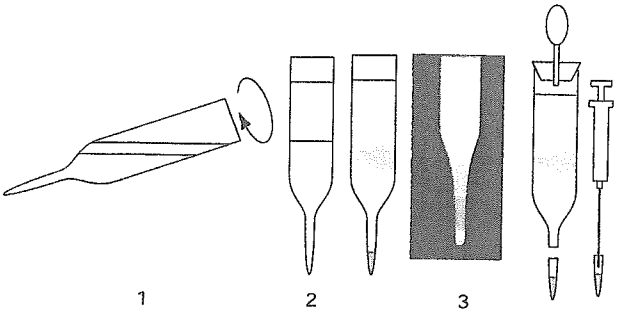

Fig. 2. Sperm fractionation in the continuous density gradient of Percoll. 1. Isotonic 90% Percoll (5.0 ml) was placed in a centrifuge tube; 1.0 ml of Hanks solution is loaded and a linear density gradient is formed by slow rotation. 2. The sperm re-suspension is layered, then centrifuged at 400 xg for 30 min. 3. The end of the test tube is cut off to recover the sediment. 4. The sperm suspension is introduced into the bottom of the culture medium to swim up. 5. Recover of swum-up sperm.

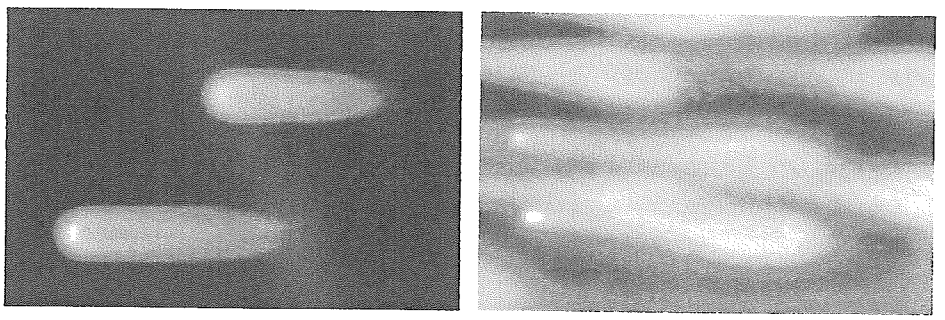

Fig. 3. Electrophoretogram of human sperm. Left: sperm with DNA integrity, Right: sperm with fragmentated DNA.

suspended in melted agarose, and a thin layer is formed on the surface derivatized glass slide. The disseminated cells are lysed with some detergent and proteinase (trypsin). Electrophoresis is performed at pH 8.4 for 10 min (2.0 V/cm voltage gradient). Figure 3 shows the electrophoretogram of human sperm. Intact sperm gives continuous DNA fibers from the origin (left photo). On the other hand, sperm with DNA fragmentation gave elongated granular particles.

Conclusion

The essence of ART is transplantation of the male chromosomes into the oocyte. Quality assurance of the sperm chromosome is, therefore, essential in not only ICSI, but also the other insemination techniques. Microscopic measurements of sperm concentration, motility and morphology may describe some aspects of the function, whereas the predictive value of these measurements is limited, even Ithough some progress has been made in recent years by the developments of the computer assisted sperm motility analyzer. In future, some molecular biological examinations of the sperm function, especially DNA integrity may play important role for the infertile therapy.

References

1) Clarke, P.G.H. (1990): Developmental cell death. Morphorogical diversity and multiple mechanisms. Anat. Embryol., 181, 195–213.
2) Eastman, A. (1993): Apoptosis: A product of programmed and unprogrammed cell death. Toxicol. Appl. Pharmacol., 121, 161–164.
3) Roosen-Runge, E.C. (1973): Germital-cell loss in normal metazoan spermatogenesis. Reprod. Fertil., 35, 339–348.
4) Sinha Hikim, A.P. and Swerdloff, R.S. (1999): Hormonal and genetic control of germ cell apoptosis in the testis. Rev. Reprod., 4, 38–47.
5) Sun, J.G., Jurisicova, A. and Casper, R.F. (1997): Detection of deoxyribonucleic acid fragmentation in human sperm: correlation with fertilization in vitro. Biol. Reprod., 56, 602–607.
6) Morris, I.D., Ilott, S., Dixon, l. and Brison, D.R. (2002): The spectrum of DNA damage in human sperm assessed by single cell gell electrophoresis (Comet assay) and its relationship to fertilization and embryo development. Human Reprod., 17, 990–998.
7) Kaneko, S., Oshio, S., Kobanawa, K., Kobayashi, T., Mhori, H. and Iizuka, R. (1986): Purification of human sperm by a discontinuous Percoll density gradient with an innercolumn. Biol. Reprod., 35, 1059–1063.
8) Kaneko, S., Sato, H., Kobanawa, K., Oshio, S., Kobayashi, T. and Iizuka, R. (1987): Continuous-step density gradient centrifugation for the selective concentration of progressively motile sperm for insemination with husband's semen. Arch. Androl., 19, 75–84.
9) Sato, H., Kaneko, S., Kobayashi, T. and Iizuka, R. (1990): Improved semen quality following a continuous-step density gradient centrifugation: its application in artificial insemination and pregnancy outcome. Arch. Androl., 24, 87–93.
10) Kaneko, S., Kobayashi, T., Oda, T., Ohno, T. and Iizuka, R. (1990): Isolation of progressively motile sperm from poor quality human semen by the modified swim down procedure. Arch. Androl., 24, 81–86.

Available online at www.sciencedirect.com
SCIENCE DIRECT®
ELSEVIER
Biochemical and Biophysical Research Communications 340 (2006) 944–952
BBRC
www.elsevier.com/locate/ybbrc

Mesenchymal progenitor cells derived from chorionic villi of +human placenta for cartilage tissue engineering

Xiaohong Zhang [a], Ayako Mitsuru [a], Koichi Igura [a], Kenji Takahashi [a], Shizuko Ichinose [b], Satoru Yamaguchi [c], Tsuneo A. Takahashi [a,*]

[a] *Division of Cell Processing, The Institute of Medical Science, The University of Tokyo (IMSUT), Tokyo, Japan*
[b] *Instrumental Analysis Research Center for Life Science, Tokyo Medical and Dental University, Tokyo, Japan*
[c] *Yamaguchi Hospital, Nishifunabashi, Funabashi, Chiba, Japan*

Received 28 November 2005
Available online 27 December 2005

Abstract

Human mesenchymal stem cells are currently being studied extensively because of their capability for self-renewal and differentiation to various connective tissues, which makes them attractive as cell sources for regenerative medicine. Herein we report the isolation of human placenta-derived mesenchymal cells (hPDMCs) that have the potential to differentiate into various lineages to explore the possibility of using these cells for regeneration of cartilage. We first evaluated the chondrogenesis of hPDMCs in vitro and then embedded the hPDMCs into an atelocollagen gel to make a cartilage-like tissue with chondrogenic induction media. For in vivo assay, preinduced hPDMCs embedded in collagen sponges were subcutaneously implanted into nude mice and also into nude rats with osteochondral defect. The results of these in vivo and in vitro studies suggested that hPDMCs can be one of the possible allogeneic cell sources for tissue engineering of cartilage.

Keywords: Placenta; Mesenchymal cells; Chondrogenesis; Cartilage; Tissue engineering

Mesenchymal stem cells from various sources are capable of differentiating into different cell lineages under proper culture conditions [1–3] and have generated a great deal of interest because of their potential use in regenerative medicine. Recently, the human placenta, umbilical cord, and amnion appeared on the stage in the search for MSCs, because of their easy availability with fewer ethical problems compared to other types of cells [4–6]. Umbilical cord blood contains high numbers of hematopoietic stem/progenitor cells and, like bone marrow, has been used to treat various hematological diseases such as leukemia and aplastic anemia, as well as inherited diseases [7,8]. Cord blood also contains mesenchymal cells and there is a report of the existence of multipotential stem cells (unrestricted somatic stem cells), though the number of MSCs is reported to be much smaller than in bone marrow, and it is also difficult to isolate them consistently [9–11]. The human placenta, umbilical cord, and amnion are discarded after the delivery of infants as medical waste. Since the information necessary for cord blood transplantation, i.e., genetic diseases in donors and their families, viral screening, contamination of microorganisms, etc, needs to be obtained by cord blood banks routinely, cells from the placenta and cord blood should be among the safest of allogeneic cell sources. HLA data such as HLA-A, -B, and -DR of the newborn are also obtained by the banks. Therefore, we chose chorionic villi from the fetal part of the human placenta as a target mesenchymal cell source.

Once cartilage is damaged, little restoration occurs because the tissue has little self-healing capacity. Many attempts have been made to repair defects of cartilage due to trauma, osteochondritis, and other conditions by

* Corresponding author. Fax: +81 3 5449 5452.
E-mail address: takahasi@ims.u-tokyo.ac.jp (T.A. Takahashi).

0006-291X/$ - see front matter © 2005 Elsevier Inc. All rights reserved.
doi:10.1016/j.bbrc.2005.12.091

transplanting chondrocytes or periosteum, and by osteochondral grafts or meniscal allografts [12–15]. However, the results were not satisfactory. The tissue engineering of cartilage has progressed significantly in recent years and bone marrow represents the main source of MSCs for both experimental and clinical studies. However, the use of these cells entails problems such as the necessity of harvesting BM from donors, individual variation [16], limitation to autologous use, and difficulty for hereditary disease patients, all of which underscore the need for alternative sources of autologous and allogeneic MSCs for medical use.

We have reported that mesenchymal progenitor cells from chorionic villi in the human placenta can differentiate into osteoblasts, chondrocytes, adipocytes, and neural cells under different induction conditions in vitro [17], and hPDMCs also have the ability to support the proliferation of hematopoietic stem cells as feeder cells [18]. Therefore, hPDMCs appear to be a possible source of MSCs for use in regenerative medicine. The aim of this study was to analyze the potential for chondrogenic differentiation of hPDMCs and examine whether the hPDMCs could be used as a source of allogeneic mesenchymal cells for tissue engineering of cartilage.

Materials and methods

Isolation and culture of human hPDMCs. This study was approved by the Institutional Review Board of IMSUT. Term placentas were collected after obtaining written informed consent from donors. The processing of the placenta started within 8 h of delivery. To isolate hPDMCs from chorionic villi, the explant culture method was used as described previously [17]. In brief, the amnion and chorionic plate were removed from the placenta, after which the fetal villi were cut into small pieces, washed thoroughly in phosphate-buffered saline (PBS), and then attached to dishes with no coating. Finally, DMEM (low glucose) with 10% FBS and 1% antibiotics/antimycotics was added to the plates. After incubation at 37 °C in a 5% CO_2 atmosphere for 2 or 3 weeks, the cells that migrated were harvested with 0.25% trypsin/1 mM EDTA solution and counted using a hemocytometer. For expansion, the harvested cells were reseeded at a density of 2×10^3 cells/cm^2 in DMEM (low glucose) with 10% FBS and 1% antibiotics/antimycotics, and the culture medium was replaced 2 times every week. The cells used in this study were within 5–15 population doublings (approximately three to six passages).

The human bone marrow-derived mesenchymal cells (hBDMCs) used in this study were purchased from BioWhittaker (Walkersville, MD) and cultured in DMEM (low glucose) with 10% FBS and 1% antibiotic/antimycotics.

Clones of hPDMCs. To analyze the chondrogeneic differentiation of subclones of hPDMCs, the cells were seeded at the density of 1×10^3 cells per 100-mm diameter dish culture in conditioned medium with 10 ng/ml recombinant human basic fibroblast growth factor (bFGF) added as a cloning medium. The culture was maintained in the cloning medium until the formation of well-defined colonies. The subclones were harvested using sterile cloning rings and expanded in the cloning medium.

Flow cytometry. The hPDMCs were harvested using a 1-mM EDTA (pH 7.4) solution. For analysis, cells were stained by combination of antibodies and propidium iodide (PI): FITC-conjugated CD44, CD31, and HLA-class I; PE-conjugated CD73, CD29, CD105, and Tie-2; APC-conjugated CD45, CD34; FITC-mouse IgG1; PE-IgG1, APC-IgG1, and PI. After exposure to labeled antibodies, cells were washed with ice-cold PBS (−) and resuspended in ice-cold PBS (−). The expression of the corresponding cell surface antigen was assayed by FACS Calibur using CELL Quest software (BD). The data were analyzed using FlowJo software (Tree Star, Ashland, OR, USA).

Pellet culture. For chondrocyte differentiation, a pellet culture system was used [19]. Briefly, 2×10^5 cells were placed in a 15-ml polypropylene tube and centrifuged into a pellet. The pellet was cultured at 37 °C with 5% CO_2 in 500 µl of chondrogenic medium containing 10 ng/ml transforming growth factor-β_3 (TGF-β_3) and 500 ng/ml bone morphogenetic protein-2 (BMP-2) in addition to high-glucose DMEM supplemented with 10^{-7} M dexamethasone, 50 µg/ml ascorbate-2-phosphate, 40 µg/ml proline, 100 µg/ml pyruvate, and 50 mg/ml ITS + Premix (6.25 µg/ml insulin, 6.25 µg/ml transferrin, 6.25 ng/ml selenious acid, 1.25 mg/ml BSA, and 5.35 mg/ml linoleic acid). The medium was replaced every 3–4 days for 21 days. The chondrogenic medium without BMP-2 was also employed. In the control, the cells were maintained in the medium without BMP-2, TGF-β_3, and dexamethasone. After 3-week induction, the pellets were embedded in paraffin and cut into 5-µm sections, which were then stained with toluidine blue. For immunohistochemistry, an anti type-II collagen monoclonal antibody was used. The reactivity was detected using a diaminobenzidine tetrahydrochloride (DAB) substrate after incubation with an HRP-linked secondary antibody.

Culture in atelocollagen gel. To examine the chondrogenic differentiation of hPDMCs in a three-dimensional culture system, the cells were cultured in atelocollagen gel (Koken, Tokyo, Japan). The volume ratio of the induction medium to 30% atelocollagen gel was 1:4, and the final cell density was adjusted to 1×10^7/ml. The cell–collagen gel composites were cultured in the chondrogenic media as described above and incubated at 37 °C with 5% CO_2. The culture medium was replaced 2 times every week. After a 3-week culture, the cell–atelocollagen gel composite was embedded in paraffin and cut into 5-µm sections for histological analysis with toluidine blue staining.

RT-PCR. To examine the cartilage-specific gene expression, total RNA was prepared from the pellet and cell–atelocollagen gel composite after induction for 2 weeks. The pellet and cell–atelocollagen gel composite were digested with 3 mg/ml collagenase for 3 and 1 h at 37 °C, respectively. hPDMCs without induction were used as a negative control. Total RNA was extracted by using Trizol-LS following the manufacturer's instructions. RT reaction was performed with a Superscript Kit for 50 min at 42 °C, followed by incubation for 15 min at 72 °C using an oligo-dT primer. For examination of the chondrogenic-related gene expression, PCR amplification was performed by 30 cycles of 94 °C for 30 s, 58 °C for 45 s, and 72 °C for 1 min. PCR products were analyzed by electrophoresis in 2% agarose gel containing ethidium bromide for visualization under UV and photographic recording. PCR primers were made as follows: Sox9 (forward) 5′-GAACGCACATCAAGACGGAG-3′, (reverse) 5′-TCTCGTTGATTTCGCTGCTC-3′ (631 bp product; Z46629); COL2A1 (forward) 5′-TTCACATATGGAGATGACAATC-3′, (reverse) 5′-AGAGTCCTAGAGTGACTGAG-3′ (472 bp product; L10347); Aggrecan (forward) 5′-AAACCACCTCTGCATTCCAC-3′, (reverse) 5′-CCTCTCTCTCCTTGCAGGTC-3′ (560 bp product; NM013227); COL10A1 (forward) 5′-CACCAGGCATTCCAGGATTCC-3′, (reverse) 5′-AGGTTGTTGGTCTGATAGCTC-3′ (926 bp product; NM009925); BMP-2 (forward) 5′-CAGAGACCC ACCCCCAGCA-3′, (reverse) 5′-CTGTTTGTGTTTGGCTTGAC-3′(688 bp product; NM007553); BMP-6 (forward) 5′-CTCGGGGTTCATAAGGTGAA-3′, (reverse) 5′- ACAGCATAAACATGGGGCTTC-3′ (412 bp product; NM001718); β-actin (forward) 5′-TGACGGGGTCACCCACACCTGTGCC-3′, (reverse) 5′-TAGAAGCATTTGCGGTGGACGATG-3′ (660 bp product; NM001101).

Transmission electron microscopic examination. The ultrastructural changes were examined by transmission electron microscopy in the pellets cultured for a week. The cultures were terminated by fixing the pellets with 2.5% glutaraldehyde in 0.1 M PBS for 2 h. The cells were washed overnight at 4 °C in the same buffer and postfixed with 1% OsO_4 buffered with 0.1 M PBS for 2 h. The pellets were dehydrated in a graded series of ethanol and embedded in Epon 812. Ultrathin sections were double-stained with uranyl acetate and lead citrate, and then examined with an H-7100 transmission electron microscope (Hitachi Hitachinaka, Japan).

Subcutaneous transplantation of hPDMC in collagen sponge into nude mice. Chondrogenesis of hPDMCs in vivo was examined by transplantation of hPDMCs into subcutaneously into nude mice. We chose the collagen sponge (5 mm in diameter by 3 mm in thickness, BD Biosciences 354513) as a scaffold to perform the in vivo experiment because it could be easily inserted did not need to be anchored by covering it with periosteum. One $\times 10^6$ cells in 100 μl medium were seeded into the collagen sponge and the composite was cultured for 2 weeks in chondrogenic medium and then transplanted into subcutaneous pockets of nude mice (5 weeks old). After 3 weeks, the composite was taken out, embedded in paraffin, and cut into 5-μm sections for histological analysis by toluidine blue staining.

Transplantation of hPDMC in collagen sponge into articular osteochondral defect in nude rats. For another experiment, a defect in articular cartilage was created as described previously [20]. Briefly, after nude rats (weight around 300 g) were anesthetized, a 3-cm-long scalp skin cut was made at the midline of the parapaellar skin. The soft tissue was dissected to expose the capsule, the capsule was incised, and the patella was dislocated laterally to expose the patella groove of the femur. A defect, 2 mm in diameter and penetrating the subchondral bone plate, was prepared on the patellar groove of the femur with a microdrill. The lesion was flushed with saline and dried with gauze. The hPDMC-loaded collagen sponge was inserted into the defect. The patella was repositioned, and the medial aspect of the capsule was closed with a nylon suture. The joint was not splinted and the rat was allowed to move freely in a cage. An empty defect served as a control. Six weeks after the surgery, the animals were sacrificed and the femoral condyles were dissected and fixed in 10% neutral-buffered formalin for 24 h. Then 0.5 M EDTA (pH 7.4) was used to decalcify the samples (for ≈7 days). The samples were paraffin-embedded, cut into 5-μm sections, and histology was examined by toluidine blue staining. The presence of human cells in the repaired tissue was confirmed by using an antibody specific for human β-2 microglobulin, a component of the class I antibody complex, as described previously [21]. In brief, the primary antibody of β-2 microglobulin conjugated with FITC was diluted 1:10 and used for staining cells. The reactivity was detected using a new fuchsin substrate system after incubation with an APL-linked anti-FITC secondary antibody.

Reagents. Culture medium and chemicals were purchased from the following companies.

Dulbecco's modified Eagle's medium (DMEM), dexamethasone, ascorbate-phosphate, proline, pyruvate, propidium iodide, and the alkaline phosphatase-conjugated anti-FITC antibody were purchased from Sigma Chemical (St. Louis, MO), fetal bovine serum (FBS) from Moregate BioTech (Bulimba, Australia), antibiotics, antimycotics, and 0.25% trypsin/1 mM EDTA solution from Gibco, Life Technologies (Grand Island, NY), Trizol-LS, oligo-dT primers, and Superscript II from Invitrogen Life Technologies (Carlsbad, CA), recombinant human BMP-2 from Yamanouchi Pharmaceutical (Tokyo, Japan), recombinant human TGF-β_3 from R&D System (Minneapolis, MN), recombinant human basic fibroblast growth factor (bFGF) from PeproTech EC (London, UK), type II collagen antibody from Lab Vision (Fremont, CA), antibodies of CD44, CD73, CD31, HLA-class I, HLA-DR, ITS+ Primix and human β_2-microglobin antibody from BD Biosciences (PharMingen, CA), antibodies of CD29, CD105, and CD34 from Beckman Coulter (Tokyo, Japan), antibody of Tie-2 from Nichirei (Tokyo, Japan), and the horseradish peroxidase (HRP)-linked antibody, new fuchsine substrate system, diaminobenzidine tetrahydrochloride (DAB) substrate, and toluidine blue solution from Dako (Kyoto, Japan).

Results

Isolation, expansion, and characterization of hPDMCs

The average number of hPDMCs that migrated per piece of chorionic villi by the explant culture method was $\approx 1 \times 10^4$ cells after 20 days and these cells had fibroblast-like shapes with a heterogeneous cell population (Fig. 1A). The phenotypes of hPDMCs were negative for hematopoietic- and endothelial-related cell antigens, such as CD31, CD34, CD45, CD133, and Tie2. They had high expression of mesenchymal progenitor-cell-related antigens, such as CD29, CD44, CD73, CD105, CD90, and HLA-class I, but not HLA-class DR (Fig. 1B). That hPDMCs were isolated without contamination by maternal cells was confirmed by XY chromosome analysis using FISH as described previously [17]. In subclonal culture, clones were isolated from culture dishes and expanded for the analysis.

Chondrocyte differentiation in pellet culture

When the hPDMCs were pelleted into a micromass and differentiated in serum-free medium in the presence of BMP-2, TGF-β_3, and dexamethasone, condensation of the pellet into a single aggregate was observed on the next day. The condensed pellet grew continuingly during culture for 3 weeks and it became white and opaque, with glistening and transparency (Fig. 2A). The pellet from the culture in the induction medium with TGF-β_3 and dexamethasone was smaller than the pellet from the culture in the medium with BMP-2 (Fig. 2B). Paraffin sections of these pellets showed that cartilage matrix was synthesized. The appearance of metachromatic matrix was demonstrated by toluidine blue staining (Fig. 2C), and type II collagen, the specific protein of chondrocyte, was demonstrated by immunohistochemical staining, indicating the occurrence of chondrogenesis.

RT-PCR was used to examine the expression of genes related to chondrogenic differentiation (Fig. 3A), such as Sox9, a major regulator of cartilage-specific genes. Expression of COL2A1, aggrecan, COL10A1, BMP-2, and BMP-6 was detected in the pellets cultured for 2 weeks. TEM examination showed that the cells in the 1-week cultured pellet were oblong with large, euchromatic, ovoid nuclei, and filled with endoplasmic reticula. These cells produced large quantities of extracellular fibers (Fig. 3B).

The pellets of cultured hBDMCs and hPDMCs were similar in size and weight after 3 weeks of induction (Figs. 4A and B). Moreover, chondrogenic differentiation analysis of subclones showed that they grew glistening and transparent (Fig. 4C), indicating that they had potential for chondrogenic differentiation.

Chondrogenic differentiation of hPDMCs in atelocollagen gel

The cell–atelocollagen gel became white, glistening, and harder than the original gel after 3 weeks of culture (Fig. 5A). In histological examination, metachromatic territorial matrixes were observed in atelocollagen gel stained by toluidine blue (Fig. 5B, top). Cells with lacuna formation were examined in the newly formed matrix (Fig. 5B, bottom). RT-PCR confirmed the expression of genes related to the chondrogenic differentiation of hPDMCs in atelocollagen gel after 2 weeks of culture (Fig. 5C).

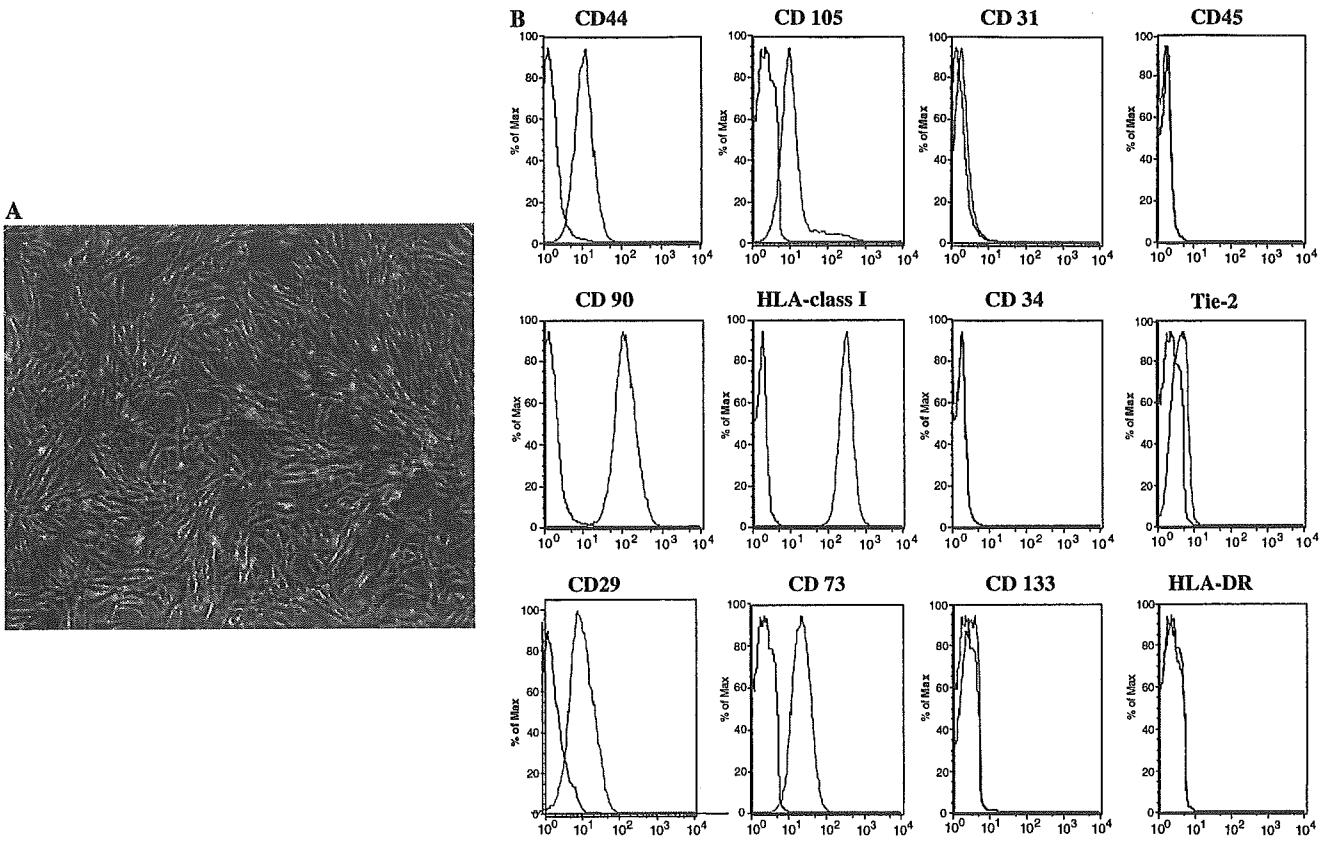

Fig. 1. Morphology of hPDMCs. (A) Proliferated cells show fibroblast-like morphology. Magnification: 40×. (B) Phenotype of hPDMCs. FACS demonstrated that the hPDMCs were positive for CD29, CD44, CD105, CD90, CD73, and HLA-class I but negative for CD31, CD34, CD45, CD133, and HLA DR.

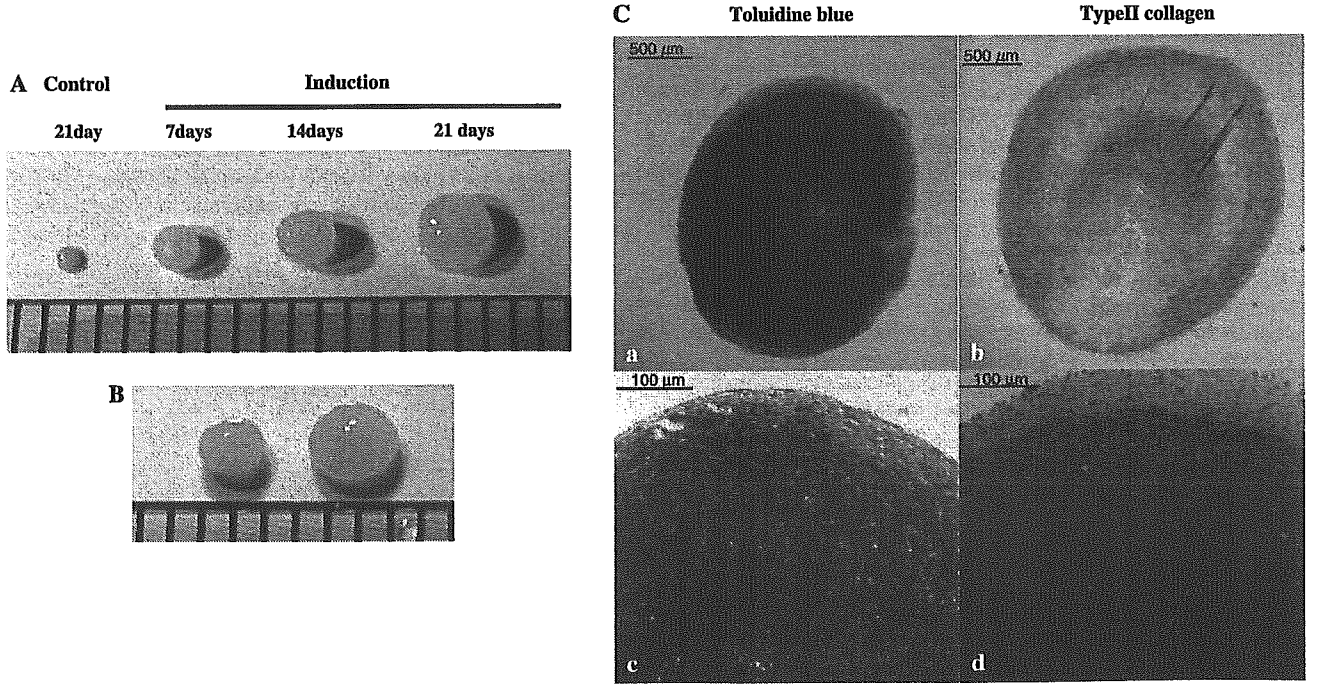

Fig. 2. Pellet culture of hPDMCs. (A) Differentiation of pellets on day 7, 14, and 21. The pellets increased in size up to 3 weeks and became white and opaque with glistening and transparency. A 1-mm scaled ruler is shown. (B) Three-week cultured pellets in the induction medium with BMP2 (right) and without BMP-2 (left). (C) Histological analysis of 3-week cultured pellets. The pellets were embedded in paraffin, sectioned, and stained with toluidine blue (a, c, and d) and the antibody for type II collagen (b). (a, b, and d) With BMP-2, (c) without BMP-2. (For interpretation of the references to colour in this figure legend, the reader is referred to the web version of this paper.)

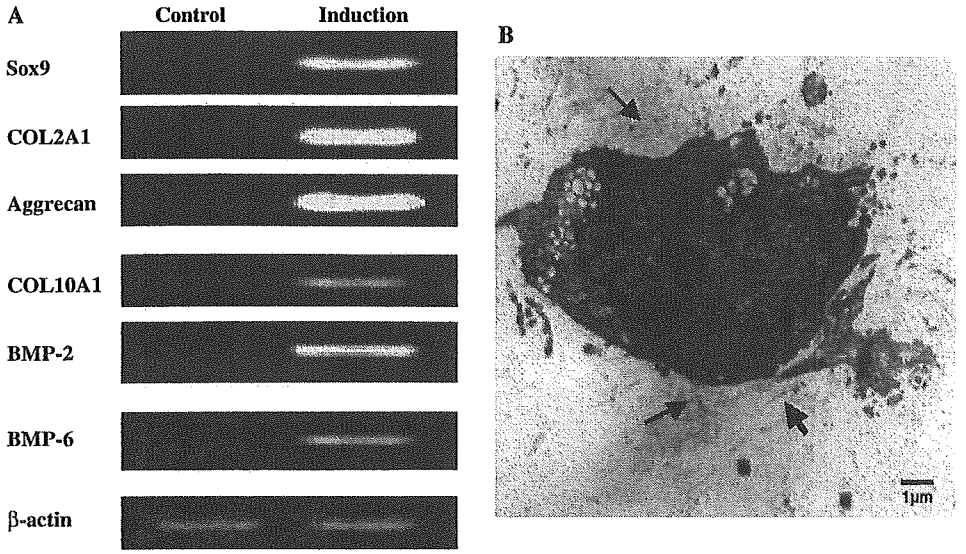

Fig. 3. RT-PCR analyses and TEM examination. (A) RT-PCR analyses for gene expression related to the chondrogenic lineage. Total RNA was extracted from pellets on day 14. Negative control was obtained from the non-induced hPDMCs. (B) TEM observation of 1-week cultured pellet. The cell is fibroblastic with an elongated, oblong phenotype having a large, euchromatic, and ovoid nucleus. The cell contains much endoplasmic reticulum. The cell produced a large number of extracellular fibers (indicated by arrows).

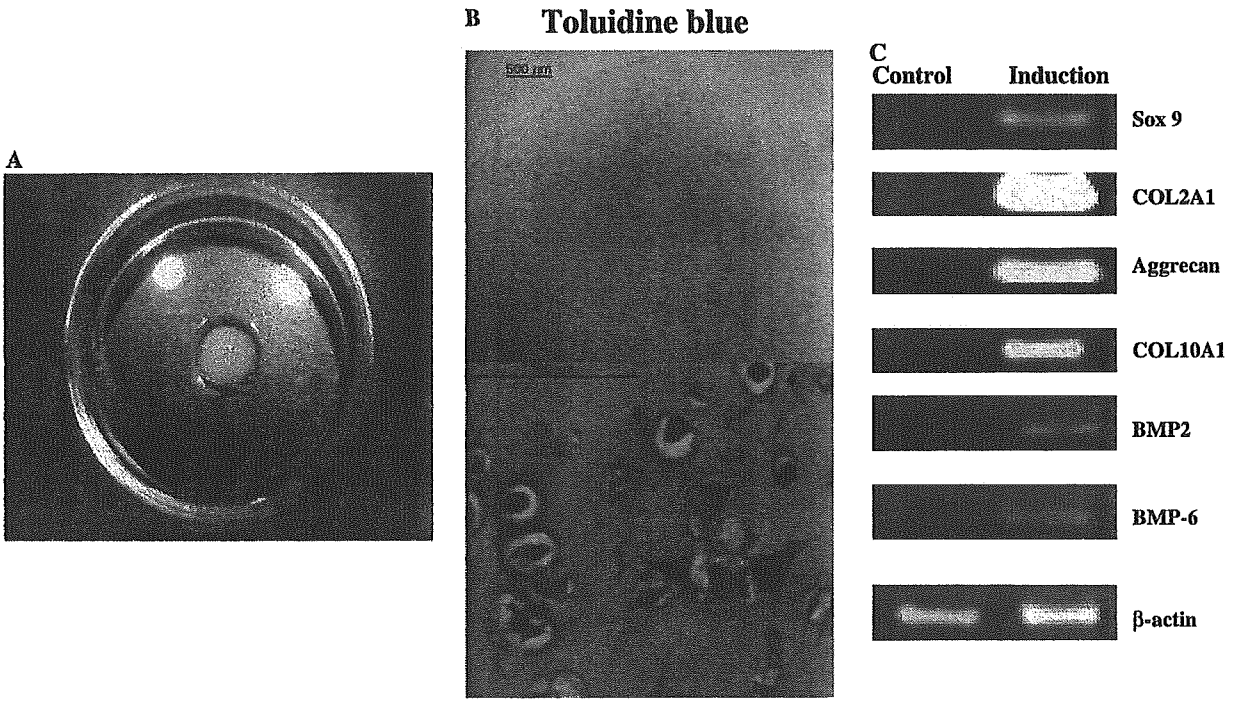

Fig. 4. Culture in atelocollagen gel. After 3-week induction, the cell–collagen gel composites (center of the picture, in a 30-mm dish) became harder than the original gel. (A) Paraffin gel section stained with toluidine blue. Metachromatic matrix was stained by toluidine blue in atelocollagen gel. In the bottom picture, the magnification of the square part, chondrocyte-like cells with formation of lacunae are shown. Top: 10×, Bottom: 250×. (B) RT-PCR confirmed the expression of genes related to chondrogenic differentiation. (For interpretation of the references to colour in this figure legend, the reader is referred to the web version of this paper.)

Chondrogenesis of hPDMCs in subcutaneous transplants

At harvest, 3 weeks after subcutaneous transplantation of the pre-induction hPDMC-loaded collagen sponges into nude mice, the composite was larger than at implantation and had changed to white and glistening, transparent stiff tissue (Fig. 6A). Chondrocyte-like cells within lacunae and a large amount of extracellular matrix were observed in the composite (Fig. 6C).

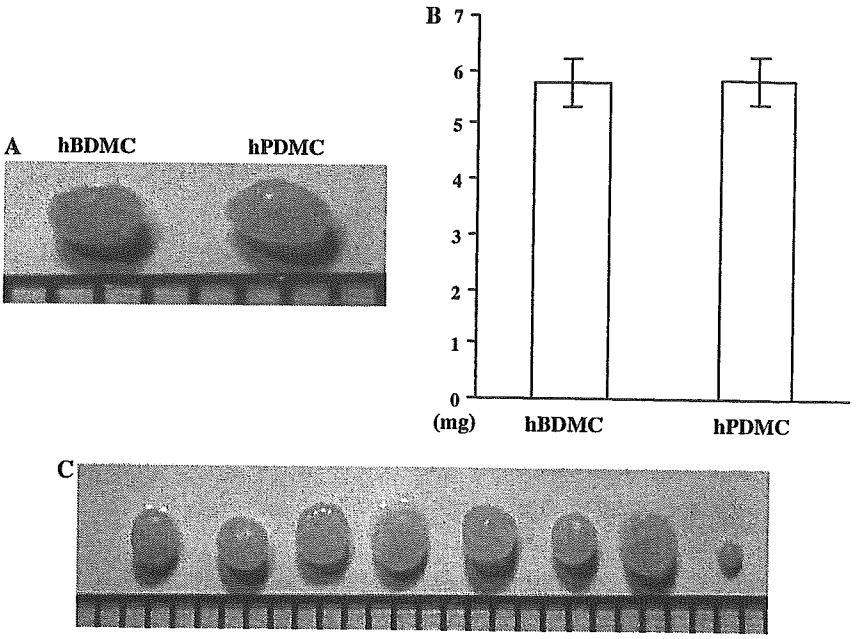

Fig. 5. Chondrogenic differentiation. (A) Pellets of hPDMCs and hBMDMCs were cultured for 21 days. A 1-mm scaled ruler is shown. (B) Weight o hPDMCs and hBMDMCs pellets on day 21. Data are showed as means ± SD ($n = 3$). (C) The clones were cultured in the cloning medium with 10 ng/m bFGF. Chondrogenic differentiation ability of clones was determined by the pellet culture at day 21. A 1-mm scaled ruler is shown. Pellets made from all clones selected increased in size and showed a glistening transparent appearance. An hPDMC pellet cultured without induction medium (right) was used a a negative control. A 1-mm scaled ruler is shown.

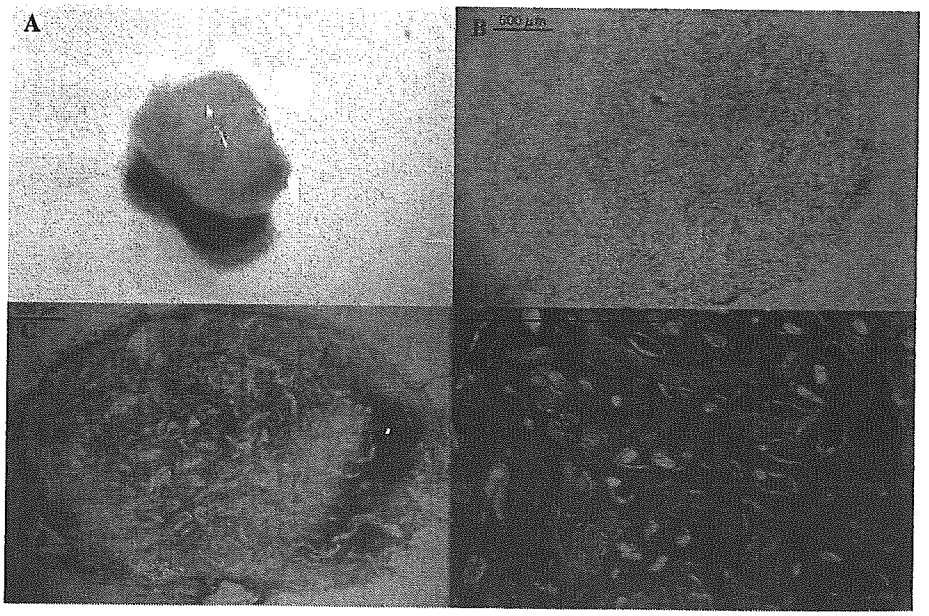

Fig. 6. In vivo chondrogenesis of hPDMCs loaded in collagen sponges in nude mice. The hPDMCs were loaded into a collagen sponge and cultured in vitro for weeks in chondrogenic medium. These sponges were implanted into subcutaneous pockets in nude mice for another 3 weeks. (A) After 3-week implantation, the PDMCs loaded in the sponge were removed from the mice. The composite was white and stiff-like cartilage tissue. (B) At 2 weeks of in vitro culture, cells filled the pores of the collagen sponge. Some local spots showed the formation of extracellular matrix detected by toluidine blue staining. (C) Histological analysis showed a large quantity of extracellular matrix formed between collagen sponge fibers in the implanted cell/collagen composite. (D) High magnification of (C). The cells are round and polygonal within the lacunae and extracellular matrix is strongly stained by toluidine blue. Magnification: (A) 2×, (B,C) 10×, and (D) 250×. (For interpretation of the references to colour in this figure legend, the reader is referred to the web version of this paper.)

Chondrogenesis of hPDMCs in osteochondral defect transplantation

In the osteochondral defect transplantation, the original defect was covered with stiff reparative tissue, which was white, and had a smooth surface at 6 weeks after surgery (Fig. 7A). Histological analysis showed that the reparative tissue filled the defect and closely adhered to the residual part of bone (Fig. 7B). All reparative regions were positive for toluidine blue. Less intense metachromatic staining was observed at the edge of the reparative tissue indicating the formation of hypertrophic cartilage. In the bottom part, the strongest metachromatic staining and round cells showed hyaline cartilage appearance. Differentiating hPDMCs in the defect were confirmed by positive staining for an antibody specific for human β_2-microglobulin (Fig. 7D).

Discussion

We isolated hPDMCs from chorionic villi of the fetal part of the human placenta at 38–40 weeks of gestation using the explant method. The surface epitopes of hPDMCs expressed mesenchymal progenitor-related antigens such as CD29, CD44, CD105, CD90, and CD73 [1,2,22,23], and were negative for hematopoietic and endothelial-related antigens such as CD31, CD45, CD34, Tie-2, and CD133. The cells expressed HLA-class I, but not HLA-DR. The hPDMCs could be differentiated into chondrocytes in induction medium with TGF-β_3 and dexamethasone, and combination with BMP-2 dramatically enhanced the production of cartilage extracellular matrix (Fig. 2B). These results were similar to those in a previous report using bone marrow and synovium-derived MSC [24,25]. RT-PCR showed expression of cartilage-specific extracellular matrix molecules (Fig. 3A), including COL2A1 and aggrecan, and the chondrogenic transcription factor Sox9 in the in vitro chondrogenesis of hPDMCs. BMP-2 and BMP-6 were expressed in culture after induction for 2 weeks, in spite of the fact that exogenous BMP-2 was provided continuously. The expression of BMP-2 and -6 has been reported in the chondrogenesis of BDMCs in vitro [24] but not in MSCs derived from synovium [25]. Endogenous BMP signals may be important for chondrogenesis of hPDMCs. Gene expression of COL10A1, a marker of hypertrophic chondrocytes, was found at 2 weeks. This was similar to the results observed during in vitro chondrogenesis of cells from bone marrow [24], adipose tissue [2], and synovium-derived MSCs in culture [25]. A similar result was also obtained from synovium-derived MSCs without BMPs [26,27]. The expression of COL10A1 seems to be characteristic of in vitro chondrogenesis of MSCs, regardless of the original tissue.

The hPDMCs could be differentiated into chondrocytes in atelocollagen gel under chondrogenic media. It has been reported that transplanting chondrocytes into a newly formed matrix of atelocollagen gel can promote restoration of the articular cartilage of the knee [28]. We attempted to

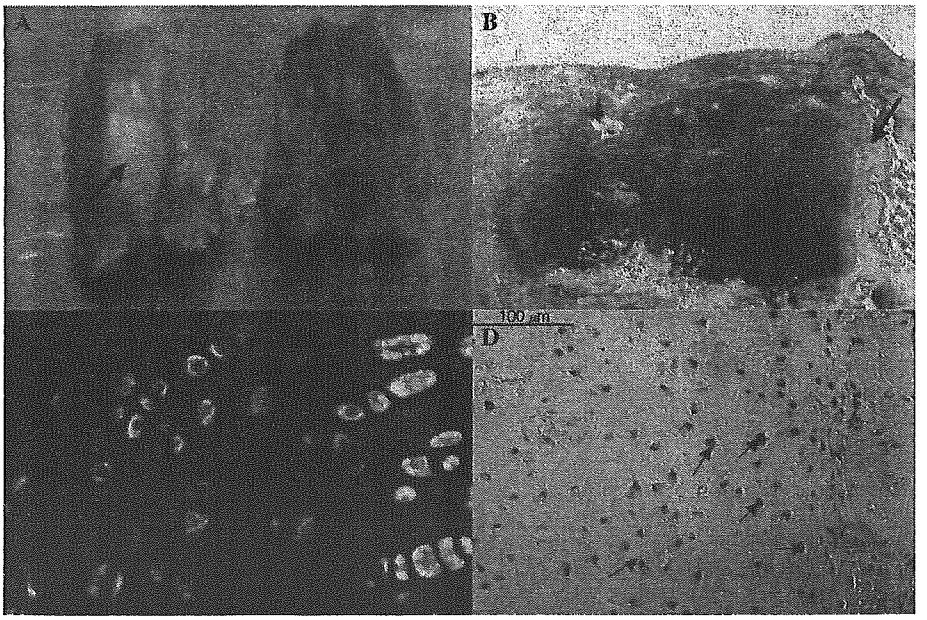

Fig. 7. Chondrogenesis of hPDMCs loaded on collagen sponge in osteochondral wound healing in a nude rat. (A) Left: The appearance of junctions of the nude rat. The hPDMCs loaded in the collagen sponge and transplanted to the defect the junction have a glass-like appearance with a smooth surface and stiffness (Arrows indicate the reparative tissue) Right: The junction where no composite was transplanted remains an empty hole. (B) Histological analysis showed that the reparative tissue filled the defect and closely adhered to the residual portion, covering all of the defect. Less intense metachromatic staining was observed at the edge of the reparative tissue. In the bottom part, round cells and high metachromasia can be observed. Arrow: junctional area between repair (left) and residual (right) part; arrowheads: collagen sponge fibers. (C) High magnification of the square in section B. Hyaline cartilage-like cells with strong metachromasia can be observed with a hyaline cartilage-like appearance. (D) Cartilage-like cells were stained with an antibody specific for human β-2 microglobulin. Arrows indicate positive cells. Magnification: (B) 10×, (C) 250×, and (D) 100×.

make cartilage-like tissue by culturing hPDMCs in atelocollagen gel and our results suggested the possibility that hPDMCs might be usable as an alternative cell source for this cellular therapy because the number of chondrocyte isolates from the knee is limited.

Transplantation of the preinduction hPDMC-loaded collagen sponge in vivo resulted in the production of cartilage with cells within lacunae surrounded by a large amount of metachromatic matrix compared to in vitro culture (Fig. 6). This indicated that differentiated hPDMCs could produce a substantial cartilage matrix in the in vivo environment. In transplantation into the osteochondral defect, reparative tissue had a cartilage-like surface and filled up the entire defect (Fig. 7A). The formation of hypertrophic repair cartilage was observed at the top part, but the bottom one had the strongest metachromasial staining and round cells, which indicated the formation of hyaline cartilage by hPDMCs (Fig. 7C). The formation of a hypertrophic cartilage surface in osteochondral defect has been reported in several clinical studies using BDMC (hypertrophic cartilage cannot function as normal hyaline cartilage and even ossification) [29,30]. Induction of mesenchymal progenitor cell differentiation into hyaline chondrocytes may be related to the potential for differentiation of the cells and induction conditions. In our investigation, the formation of hyaline cartilage in the bottom part of the reparative tissue indicated the possibility that hPDMCs could be used for repairing damaged articular cartilage. Therefore, appropriate induction conditions and a good experimental model are needed to examine the redevelopment of the articular surface as well as the formation of subchondral bone in osteochondral defect repair by hPDMCs.

According to a previous report, the pellet's size and weight are convincing indicators for in vitro chondrogenesis of MSCs [25], Our data showed that the chondrogenesis potential of hPDMCs was comparable to that of hBDMCs (Figs. 4A and B). Clonal analysis showed that the population of hPDMCs was homogeneous after several passages, because the potential for chondrogenic differentiation was evident in the examined clones (Fig. 4C). However, we found that chondrogenic differentiation potential differed in individual hPDMCs, perhaps depending on the individual cell or primary cells that randomly migrated from placental tissue pieces. Thus, an effective method to isolate mesenchymal progenitor cells from the placenta and to identify-specific surface markers of stem cells and progenitors of mesenchymal cells in hPDMC is necessary.

Recently, it has been reported that human mesenchymal stem cells modulate allogeneic immune cell responses [31–33]. If so, and if hPDMCs can differentiate into chondrocytes in vitro and in vivo, they will be one of the possible cell sources for cartilage tissue engineering. However, further studies remain necessary to precisely analyze the chondrogenesis of hPDMCs and to explore potential methods for clinical application.

Acknowledgments

This work was partially supported by a research gran on Human Genome, Tissue Engineering (H17-014) fror the Japanese Ministry of Health, Labor and Welfare. W thank Yamanouchi Pharmaceutical Co., Ltd. for the kin gift of rhBMP-2.

References

[1] M.F. Pittenger, A.M. Mackay, S.C. Beck, R.K. Jaiswal, R. Douglas J.D. Mosca, M.A. Moorman, D.W. Simonetti, S. Craig, D.R Marshak, Multilineage potential of adult human mesenchymal ster cells, Science 284 (1999) 143–147.

[2] P.A. Zuk, M. Zhu, P. Ashjian, D.A. De Ugarte, J.I. Huang, H Mizuno, Z.C. Alfonso, J.K. Fraser, P. Benhaim, M.H. Hedrick Human adipose tissue is a source of multipotent stem cells, Mol. Biol Cell 13 (2002) 4279–4295.

[3] G. Kogler, S. Sensken, J.A. Airey, T. Trapp, M. Muschen, N Feldhahn, S. Liedtke, R. Sorg, J. Fischer, C. Rosenbaum, S Greschat, A. Knipper, J. Bender, O. Degistirici, J. Gao, A. Caplan E.J. Colletti, G. Almeida-Porada, H.W. Muller, E. Zanjani, P Wernet, A new human somatic stem cell from placental cord blood with intrinsic pluripotent differentiation potential, J. Exp. Med. 200 (2004) 123–135.

[4] N. Ochsenbein-Kolble, G. Bilic, H. Hall, R. Huch, R. Zimmermann Inducing proliferation of human amnion epithelial and mesenchyma cells for prospective engineering of membrane repair, J. Perinat. Med 31 (2003) 287–294.

[5] S. Fu, Y.C. Cheng, M.Y. Lin, H. Cheng, P.M. Chu, S.C. Chou, Y.H Shih, M.H. Ko, M.S. Sung, Conversion of human umbilical mesenchymal stem cells in Wharton's jelly to dopaminergic neurons in vitro potential therapeutic application for Parkinsonism, Stem Cells (2005) [Epub ahead of print].

[6] D. Li, W.Y. Zhang, H.L. Li, X.X. Jiang, Y. Zhang, P. Tang, N. Mao Isolation and identification of a multilineage potential mesenchyma cell from human placenta, Placenta (2005), Sep 17 [Epub ahead of print].

[7] J. Kurtzberg, M. Laughlin, M.L. Graham, C. Smith, J.F. Olson, E.C Halperin, G. Ciocci, C. Carrier, C.E. Stevens, P. Rubinstein, Placental blood as a source of hematopoietic stem cells for transplantation into unrelated recipients, N. Engl. J. Med. 335 (1996) 157–166.

[8] E. Gluckman, Hematopoietic stem-cell transplants using umbilical-cord blood, N. Engl. J. Med. 344 (2001) 1860–1861.

[9] J. Kang, J.E. Yeom, H.J. Lee, S.H. Rho, H. Han, G.T. Chae, Growth kinetics of human mesenchymal stem cells from bone marrow and umibilical cord blood, Acta Haematol. 112 (2004) 230–233.

[10] K. Bieback, S. Kern, H. KlÜter, H. Eichler, Critical parameters for the isolation of mesenchymal stem cells from umbilical cord blood, Stem Cells 634 (2004) 625–634.

[11] W. Wagner, F. Wein, A. Seckinger, M. Frankhauser, U. Wirkner, U. Krause, J. Blake, C. Schwager, V. Eckstein, W. Ansorge, A.D. Ho, Comparative characteristics of mesenchymal stem cells from human bone marrow, adipose tissue, and umbilical cord blood, Exp. Hematol. 33 (2005) 1402–1416.

[12] A.P. Newman, Articular cartilage repair, Am. J. Sports Med. 26 (1998) 309–324.

[13] V.E. Hoikka, H.J. Jaroma, V.A. Ritsila, Reconstruction of the patellar articulation with periosteal grafts. 4-year follow-up of 13 cases, Acta Orthop. Scand. 61 (1990) 36–39.

[14] D. Amiel, R.D. Coutts, M. Abel, W. Stewart, F. Harwood, W.H. Akeson, Rib perichondrial graft for the repair of full-thickness articular-cartilage defects. A morphological and biochemical study in rabbits, J. Bone Joint Surg. 67 (1985) 175–180.

[15] M. Brittberg, A. Lindahl, A. Nilsson, C. Ohlsson, O. Isaksson, L. Peterson, Treatment of deep cartilage defects in the knee with autologous chondrocyte transplantation, N. Engl. J. Med. 331 (1994) 889–895.
[16] M.S. Rao, M.P. Mattson, Stem cells and aging: expanding the possibilities, Mech. Ageing Dev. 122 (2001) 713–734.
[17] K. Igura, X. Zhang, K. Takahashi, A. Mitsuru, S. Yamaguchi, T.A. Takahashi, Isolation and characterization of mesenchymal progenitor cells from chorionic villi of human placenta, Cytotherapy 6 (2004) 543–553.
[18] Y. Zhang, C. Li, X. Jiang, S. Zhang, Y. Wu, B. Liu, P. Tang, N. Mao, Human placenta-derived mesenchymal progenitor cells support culture expression of long-term culture-initiating cells from cord blood $CD34^+$ cells, Exp. Hematol. 32 (2004) 657–664.
[19] B. Johnstone, T.M. Hering, A.I. Caplan, V.M. Goldberg, J.U. Yoo, In vitro chondrogenesis of bone marrow-derived mesenchymal progenitor cells, Exp. Cell Res. 238 (1998) 265–272.
[20] T. Nishida, S. Kubota, S. Kojima, T. Kuboki, K. Nakao, T. Kushibiki, Y. Tabata, M. Takagawa, Regeneration of defects in articular cartilage in rat knee joints by CCN2 (connective tissue growth factor), J. Bone Miner. Res. 19 (2004) 1308–1319.
[21] K.W. Liechty, T.C. Mackenzie, A.F. Shaaban, A. Radu, A.B. Moseley, R. Deans, D.R. Marshak, A.W. Flak, Human mesenchymal stem cells engraft and demonstrate site-specific differentiation after in utero transplantation in sheep, Nat. Med. 6 (2000) 1282–1286.
[22] P.A. Conget, J.J. Minguell, Phenotypical and functional properties of human bone marrow mesenchymal progenitor cells, J. Cell. Physiol. 181 (1999) 67–73.
[23] S. Gronthos, D.M. Franklin, H.A. Leddy, P.G. Robey, R.W. storms, J.M. Gimble, Surface protein characterization of human adipose tissue-derived stromal cells, J. Cell. Physiol. 189 (2001) 54–63.
[24] I. Sekiya, J.T. Vuoristo, B.L. Larson, D.J. Prockop, In vitro cartilage formation by human adult stem cells from bone marrow stroma defines the sequence of cellular and molecular events during chondrogenesis, Proc. Natl. Acad. Sci. USA 99 (2002) 4397–4402.
[25] S. Shirasawa, I. Sekiya, Y. Sakaguchi, K. Yagisha, S. Ichinose, T. Muneta, In vitro chondrogenesis of human synovium-derived mesenchymal stem cells: optimal condition and comparison with bone marrow-derived cells, J. Cell. Biochem. (2005). Aug 8 [Epub ahead of print].
[26] K. Nishimura, L.A. Solchaga, A.I. Caplan, J.U. Yoo, B. Johnstone, Chondroprogenitor cells of synovial tissue, Arthritis Rheum. 42 (1999) 2631–2637.
[27] C. De Bari, F. Dell' Accio, P. Tylzanowski, F.P. Luyten, Mulitpotent mesenchymal stem cells from adult human synovial membrane, Arthritis Rheum. 44 (2001) 1928–1942.
[28] M. Ochi, Y. Uchio, K. Kawasaki, S. Wakitani, J. Iwasa, Transplantation of cartilage-like tissue made by tissue engineering in treatment of cartilage defect of the knee, J. Bone Joint Surg. 84 (2002) 571–578.
[29] S. Wakitani, K. Imoto, T. Yamamoto, M. Saito, N. Murata, M. Yoneda, Human autologous culture expanded bone marrow mesenchymal cell transplantation for repair of cartilage defects in osteoarthritic knees, Osteoarthritis Cartilage 10 (2002) 199–206.
[30] M. Radice, P. Brum, R. Cortive, R. Scapinelli, C. Battaliard, G. Abatangelo, Hyaluronan-based biopolymers as delivery vehicles for bone-marrow-derived mesenchymal progenitors, J. Biomed. Mater. Res. 50 (2000) 101–109.
[31] O.N. Koc, J. Day, M. Nieder, S.L. Gerson, H.M. Lazarus, W. Krivit, Allogeneic mesenchymal stem cell infusion for treatment of metachromatic leukodystrophy (MLD) and Hurler syndrome (MPS-IH), Bone Marrow Transplant. 30 (2002) 215–222.
[32] E.M. Horwitz, P.L. Gordon, W.K. Koo, J.C. Marx, M.D. Neel, R.Y. McNall, L. Muul, T. Hofman, Isolated allogeneic bone marrow-derived mesenchyal cells engraft and stimulate growth in children with osteogenesis imperfecta: implications for cell therapy of bone, Proc. Natl. Acad. Sci. USA 99 (2002) 8932–8937.
[33] K. Le Blanc, I. Rasmusson, B. Sundberg, C. Gotherstrom, M. Hassan, M. Uzuuel, O. Ringden, Treatment of severe acute graft-versus host disease with third party haploidentical mesenchymal stem cells, Lancet 363 (2004) 1439–1441.

European Journal of Immunology

Expansion of Vα24$^+$Vβ11$^+$ NKT cells from cord blood mononuclear cells using IL-15, IL-7 and Flt3-L depends on monocytes

Hikaru Okada[*1], *Tokiko Nagamura-Inoue*[1,2], *Yuka Mori*[1] *and Tsuneo A. Takahashi*[1]

[1] Division of Cell Processing, Research Hospital, Institute of Medical Science, University of Tokyo, Tokyo, Japan
[2] Department of Cell Processing and Transfusion, Research Hospital, Institute of Medical Science, University of Tokyo, Tokyo, Japan

Human Vα24$^+$Vβ11$^+$ NKT cells are a unique T cell population specifically and potently activated by α-galactosylceramide (αGalCer; KRN7000) presented by CD1d. Here, we present a simple and efficient method for expanding Vα24$^+$Vβ11$^+$ NKT cells from human cord blood mononuclear cells (CBMNC) using αGalCer in the presence of interleukin (IL)-15, IL-7 and Flt3-L. The addition of αGalCer from day 0, compared to its addition from day 8 or day 15, induced a greater expansion of NKT cells. The maximal expansion of NKT cells was observed after 15 days (2300-fold). Thereafter, the number of NKT cells decreased slowly, a decrease that was correlated with the diminution of CD1d-positive cells. NKT cell proliferation induced by αGalCer was not observed when CD1d-expressing monocytes were depleted from CBMNC, whereas B cell and dendritic cell depletions had no effect. Expanded NKT cells were CD4$^+$CD8$^-$ and secreted both IL-4 and IFN-γ. In this system, CD3$^+$ T cells and CD3$^-$CD56$^+$ NK cells were also expanded. However, the expansion of NKT cells had no significant functional effect on T and NK cells. This expansion method of CBMNC-derived NKT cells is simple and may be helpful for clinical use.

Received 9/2/05
Revised 15/9/05
Accepted 9/11/05

[DOI 10.1002/eji.200526085]

Key words: α-Galactosylceramide · Cord blood · Expansion · Human · Vα24$^+$Vβ11$^+$ NKT cells

Introduction

Natural killer T (NKT) cells correspond to a novel T cell population with an invariant TCR that recognizes glycolipids presented by CD1d, an MHC-like molecule well conserved between humans and mice [1–3]. Many studies have described the potential anti-tumor effect [4–7] and the immunoregulatory function of NKT cells [8–11]. Vα24$^+$Vβ11$^+$ NKT cells, the human counterpart of mouse Vα14$^+$Vβ8.2$^+$ NKT cells, are limited to a small lymphocyte subpopulation [12] that can be selectively activated by α-galactosylceramide (αGalCer; KRN7000) presented by CD1d [13, 14]. Takahashi *et al.* and others showed that they proliferate in response to dendritic cells (DC) once pulsed by αGalCer [15, 16]. Several cytokines were used in attempt to expand and activate NKT cells from human peripheral blood [17–19], and recently from human cord blood [20, 21]. Interleukin (IL)-2 is one of the classical cytokines used to expand and stimulate NKT cells [22]. Here, we describe a

Correspondence: Tsuneo A. Takahashi, Division of Cell Processing, Institute of Medical Science, University of Tokyo, 4-6-1, Shirokanedai, Minato-ku, Tokyo, 108–8639, Japan
Fax: +81-3-54495452
e-mail: takahasi@ims.u-tokyo.ac.jp

Abbreviations: αGalCer: α-galactosylceramide · **βGalCer:** β-galactosylceramide · **CBMNC:** cord blood mononuclear cell · **CBT:** cord blood transplantation · **GVHD:** graft-*versus*-host disease · **GVL:** graft-*versus*-leukemia

* Current address: Central Laboratory of Hematology, Centre Hospitalier Universitaire Vaudois, Bugnon 46, 1011 Lausanne, Switzerland.

Table 1. Cell compartments of CBMNC before and after culture[a)]

Cord Blood	T cells ($CD3^+$)	NK cells	B cells	Monocytes	DC
Day 0	15.0 ± 9.6	19.9 ± 10.3	10.2 ± 4.4	32.4 ± 7.6	0.04 ± 0.02
Day 8	74.6 ± 8.1	20.7 ± 8.2	2.16 ± 0.01	0.16 ± 0.01	0.11 ± 0.01
Day 15	86.2 ± 8.6	13.1 ± 9.0	ND	ND	ND

[a)] Cells were cultured in the presence of 50 ng/mL IL-15, 10 ng/mL IL-7, 10 ng/mL Flt3-L and 100 ng/mL αGalCer from day 0. Data shown are the means ± SD of ten samples (% of CBMNC). ND: not determined.

combination of IL-15, IL-7 and Flt3-ligand (Flt3-L) to expand NKT cells from human cord blood mononuclear cells (CBMNC). IL-15 is a newly cloned cytokine that promotes T cell proliferation and NK cell activation [23]. In fact, in IL-$15^{-/-}$ and IL-$15R\alpha^{-/-}$ mice, NK and NKT cell counts are diminished [24, 25]. IL-7 is a potent lymphoid growth factor that is important for T cell proliferation and survival as well as for NK cell function [26]. Flt3-L induces hematopoietic stem cell proliferation and early lymphopoiesis. In addition, we have previously shown that a high concentration of IL-15 (50 ng/mL), together with 10 ng/mL of Flt3-L, efficiently expands $CD3^+$ T cells derived from human CBMNC [27].

Cord blood is a source of stem cells currently used for transplantation. Several aspects of unrelated cord blood transplantation (CBT) differ from bone marrow or peripheral blood stem cell transplantation. As many as two HLA mismatches are acceptable in CBT for successful engraftment with only a mild graft-*versus*-host disease (GVHD) [28], because cord blood T cells are immature and naive compared to peripheral blood lymphocytes. The relationship between lower risk of GVHD and higher risk of leukemic relapse is well known, and a higher risk of relapse in CBT was expected. Surprisingly, unrelated CBT and unrelated bone marrow transplantation had a comparable relapse rate in adults as well as in children [29, 30]. However, the major causes of death in CBT in adults were relapse of the disease and infections due to delayed hematopoietic recovery [30, 31]. As $V\alpha24^+V\beta11^+$ NKT cells produce both Th1 and Th2 cytokines upon activation, they may have an immunomodulatory effect that could abolish GVHD without affecting the graft-*versus*-leukemia (GVL) effect [32, 33].

Here, we present a simple and efficient method for expanding $V\alpha24^+V\beta11^+$ NKT cells derived from human CBMNC. Moreover, we observed that monocytes are critical for $V\alpha24^+V\beta11^+$ NKT cell expansion. Expansion of T lymphocytes and NK cells was also observed. Expanded $V\alpha24^+V\beta11^+$ NKT cells had a $CD4^+CD8^-$ phenotype and secreted both IL-4 and IFN-γ. Observations presented here may be helpful for a more targeted use of human cord blood in immunotherapy.

Results

Phenotypic analysis of lymphocytes in human cord blood

After separation by Ficoll density gradient centrifugation, $CD3^+$ T cells varied in fresh CBMNC from 2.5 to 36.2% (mean 15.0 ± 9.6%, n = 10). Other cell compartments consisted of 19.9 ± 10.3% $CD3^-CD56^+$ NK cells, 10.2 ± 4.4% $CD19^+$ B cells, 32.4 ± 7.6% $CD14^+$ monocytes and only 0.04 ± 0.02% $CD3^-CD1a^+$ DC as shown in Table 1 (day 0). The majority of $CD3^+$ T cells were $TCR\alpha\beta^+$ (97.0 ± 2.1%) and 3.0 ± 2.1% were $TCR\gamma\delta^+$. Of T cells, 75.8 ± 14.1% were $CD4^+CD8^-$ (CD4 single-positive cells), 18.2 ± 9.5% $CD4^-CD8^+$ (CD8 single-positive cells), 2.5 ± 2.5% $CD4^+CD8^+$ (double-positive cells) and 1.1 ± 0.9% $CD4^-CD8^-$ (double-negative cells) (Table 2, day 0). Only 0.04 ± 0.03% of $CD3^+$ T cells were $V\alpha24^+V\beta11^+$ NKT cells (Table 2).

Cytokine combination for cell expansion

Because NKT cells, and especially $V\alpha24^+V\beta11^+$ NKT cells, represent a very small population of T cells, we

Table 2. T cell phenotypes in CBMNC before and after culture[a)]

	$TCR\alpha\beta^+$	$TCR\gamma\delta^+$	$CD4^+CD8^-$	$CD4^-CD8^+$	$CD4^+CD8^+$	$CD4^-CD8^-$	$V\alpha24^+V\beta11^+$ NKT
Day 0	97.0 ± 2.1	3.0 ± 2.1	75.8 ± 14.1	18.2 ± 9.5	2.5 ± 2.5	1.1 ± 0.9	0.04 ± 0.03
Day 8	95.2 ± 0.8	5.3 ± 1.4	66.1 ± 12.1	29.6 ± 10.7	0.6 ± 0.1	3.7 ± 1.8	0.8 ± 0.6
Day 15	91.9 ± 1.6	8.0 ± 0.9	60.8 ± 9.6	31.4 ± 11.2	4.4 ± 1.1	3.4 ± 0.5	3.7 ± 0.3

[a)] Cells were cultured under the same condition as in Table 1. Data shown are the means ± SD of six samples (% of $CD3^+$ T cells).

chose to expand CBMNC rather than sorting $V\alpha24^+V\beta11^+$ NKT cells. Previously, Nagamura-Inoue *et al.* found that a high concentration of IL-15 (50 ng/mL), together with 10 ng/mL Flt3-L, efficiently expanded $CD3^+$ T cells derived from CBMNC [27]. In addition, IL-7 is one of the growth factors needed to expand and activate T cells [26]. Therefore, we compared different combinations of these three cytokines (50 ng/mL IL-15, 10 ng/mL IL-7 and/or 10 ng/mL Flt3-L). Results are shown in Fig. 1. In the absence of cytokines or in the presence of Flt3-L alone, $CD3^+$ T cells and NK cells diminished by day 15, and the remaining cells were $CD3^-CD56^-$. IL-7 at 10 ng/mL only resulted in 2.3-fold expansion of T cells. A significant synergistic induction of $CD3^+$ T cells was observed with a combination of 50 ng/mL IL-15, 10 ng/mL IL-7 and 10 ng/mL Flt3-L (14.1-fold induction). However, even by combining these three cytokines, no increase of $V\alpha24^+V\beta11^+$ NKT cells was observed unless αGalCer was added.

CD1d-expressing cells in human cord blood

Since $V\alpha24^+V\beta11^+$ NKT cell activation is CD1d dependent, we examined whether antigen-presenting cells like monocytes ($CD14^+$), B cells ($CD19^+$) and DC ($CD3^-CD1a^+$) expressed CD1d in fresh CBMNC. As shown in Fig. 2A, the majority of CD1d-positive cells were observed among $CD14^+$ monocytes, whereas $CD19^+$ B cells did not strongly express CD1d and only 0.01% of $CD3^-CD1a^+$ DC were $CD1d^+$ among human CBMNC. By day 8 in the presence of IL-15, IL-7 and Flt3-L, $CD1d^+$ cells decreased as shown in Table 1 (day 8). In addition, the remaining B cells, monocytes and the few DC no longer expressed CD1d (Fig. 2A, right panels).

Expansion of NKT cells from human cord blood

IL-15 is a cytokine that has been reported to induce monocyte differentiation into mature DC [34]. In order to explore whether DC maturation could enhance $V\alpha24^+V\beta11^+$ NKT cell expansion, αGalCer was directly added to CBMNC cultured with IL-15, IL-7 and Flt3-L from day 0, day 8 or day 15. The addition of αGalCer from day 0 induced a significantly greater $V\alpha24^+V\beta11^+$ NKT cell expansion than the addition of αGalCer from day 8 or day 15 (Fig. 2B). After 15 days of culture, the absolute number of $V\alpha24^+V\beta11^+$ NKT cells pulsed with αGalCer was 2300 ± 1200-fold higher than that observed in fresh CBMNC (Fig. 2B). $CD3^+$ T cells and NK cells were also expanded 27 ± 15-fold and 2 ± 1-fold, respectively, compared to the pre-cultured population (Fig. 2C). $CD3^+$ T cells and NK cells represent 86.2 ± 8.6% and 13.1 ± 9.0%, respectively, of total cultured CBMNC on day 15 (Table 1, day 15). In control experiments, β-galactosylceramide (βGalCer) did not induce $V\alpha24^+V\beta11^+$ NKT cell proliferation, while the T cells or NK cells presented almost the same expansion rate. As described above, the $CD3^-CD56^-$ fraction nearly disappeared on day 8 (Fig. 2C). Maximal expansion of $V\alpha24^+V\beta11^+$ NKT cells was observed after 15 days of culture. Thereafter, the absolute number of $V\alpha24^+V\beta11^+$ NKT cells slowly decreased, a phenomenon that followed the reduction of $CD1d^+$ cells (Table 1, Fig. 2A).

Depletion of antigen-presenting cells

Because $V\alpha24^+V\beta11^+$ NKT cells could only be expanded in the presence of αGalCer, we next tried to detect which $CD1d^+$ cells in the CBMNC were critical for the

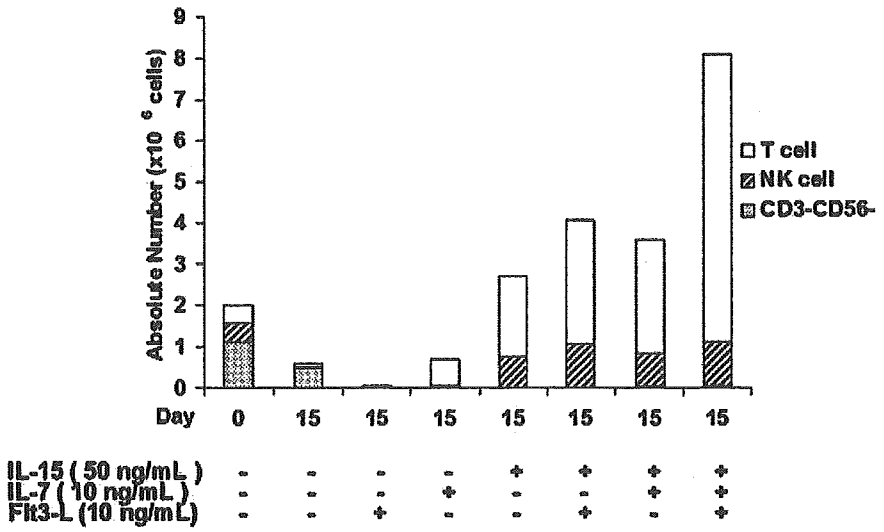

Figure 1. Comparison of cell compartments in fresh CBMNC (day 0) and after 15 days of culture with different combinations of 50 ng/mL IL-15, 10 ng/mL IL-7 and 10 ng/mL Flt3-L.

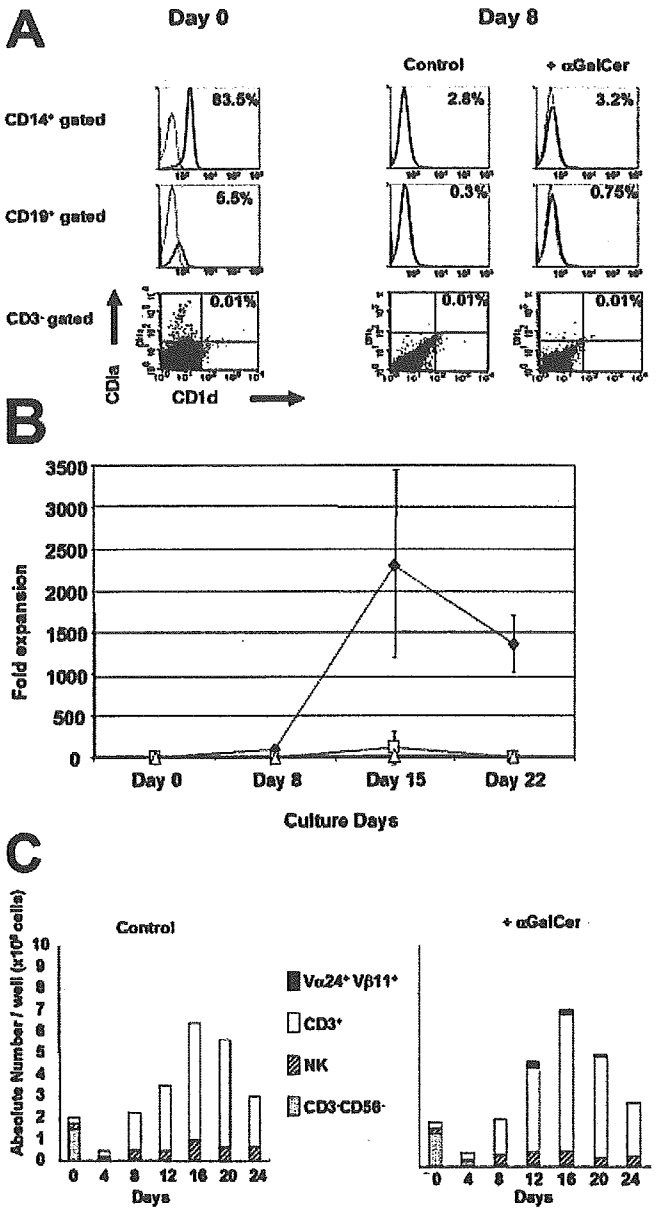

Figure 2. (A) CD1d expression on $CD14^+$ monocytes, $CD19^+$ B cells and $CD3^-CD1a^+$ DC in freshly isolated CBMNC (left panel, day 0) and after 8 days of culture with 50 ng/mL IL-15, 10 ng/mL IL-7 and 10 ng/mL Flt3-L in the presence or absence of αGalCer from day 0 (right panels, day 8). Isotype control is represented with a dashed line and CD1d-positive cells with a solid line for $CD14^+$- and $CD19^+$-gated cells. $CD3^-$ cells are gated in the dot blots and $CD3^-CD1a^+CD1d^+$ cells represented only 0.01% of the $CD3^-CD1a^+$ cells. (B) Fold expansion of $V\alpha24^+V\beta11^+$ NKT cells. αGalCer (100 ng/mL) was added to the CBMNC from day 0 (◆), day 8 (□) or day 15 (△) in the presence of 50 ng/mL IL-15, 10 ng/mL IL-7 and 10 ng/mL Flt3-L. The fold expansion represents the ratio of the absolute number of NKT cells per well after culture to the number at day 0. (C) Cell compartments of CBMNC in the presence or absence of αGalCer. CBMNC were cultured with 50 ng/mL IL-15, 10 ng/mL IL-7 and 10 ng/mL Flt3-L. αGalCer was added to the medium at a concentration of 100 ng/mL from day 0 (right panel). βGalCer was used in a control experiment (left panel).

expansion of $V\alpha24^+V\beta11^+$ NKT cells. CBMNC were depleted of either $CD14^+$ monocytes, $CD19^+$ B cells, $CD1a^+$ DC, or of all of these three antigen-presenting cells. Then, depleted cells were individually cultured in the presence of IL-15, IL-7 and Flt3-L as described above and pulsed with 100 ng/mL αGalCer from day 0. The absolute number of $V\alpha24^+V\beta11^+$ NKT cells was calculated as described in Materials and methods. When $CD14^+$ monocytes were depleted, the $V\alpha24^+V\beta11^+$ NKT cells did not proliferate, as shown in Fig. 3. In contrast, depletion of $CD19^+$ B cells or $CD1a^+$ DC had no significant influence on the proliferation of $V\alpha24^+V\beta11^+$ NKT cells.

Phenotypic analysis of expanded $V\alpha24^+V\beta11^+$ NKT cells and $CD3^+$ T cells

CBMNC were cultured with IL-15, IL-7, Flt3-L and 100 ng/mL αGalCer. After 15 days, $CD3^+$ T cells represented 86.2 ± 8.6% of the mononuclear cells and the remaining population was constituted by NK cells (13.1 ± 9.0%) (Table 1). Expanded $V\alpha24^+V\beta11^+$ NKT cells represented 3.7 ± 0.3% of the $CD3^+$ T cells (Fig. 4A, lower part). Most of the $V\alpha24^+$ NKT cells were positive for CD4 (95.6 ± 5.1%) and very few expressed CD8 (1.1 ± 1.1%) (n = 5). In addition, 1.8% $V\alpha24^+$ NKT cells were double negative ($CD4^-CD8^-$). Of the other $CD3^+$ T cells in cultured cells, 60.8 ± 9.6% were $CD4^+$, 31.4 ± 11.2% $CD8^+$, 4.4 ± 1.1% $CD4^+CD8^+$, 3.4 ± 0.54% $CD4^-CD8^-$ (Table 2, day 15) and 23.8 ± 7.9% of $CD3^+$ T cells were $CD56^+$ (n = 6). In the absence of αGalCer, $V\alpha24^+V\beta11^+$ NKT cells were not

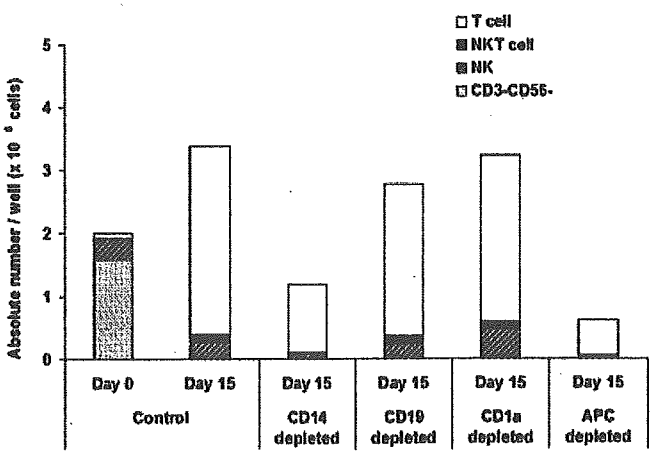

Figure 3. Depletion of CD1d-expressing cells. Either $CD14^+$ monocytes, $CD19^+$ B cells, $CD1a^+$ DC or all of these three antigen-presenting cells (APC) were depleted from CBMNC using AutoMACS beads. After depletion, the remaining cells were cultured with 50 ng/mL IL-15, 10 ng/mL IL-7, 10 ng/mL Flt3-L and 100 ng/mL αGalCer for 15 days. One representative result from three independent experiments is shown.

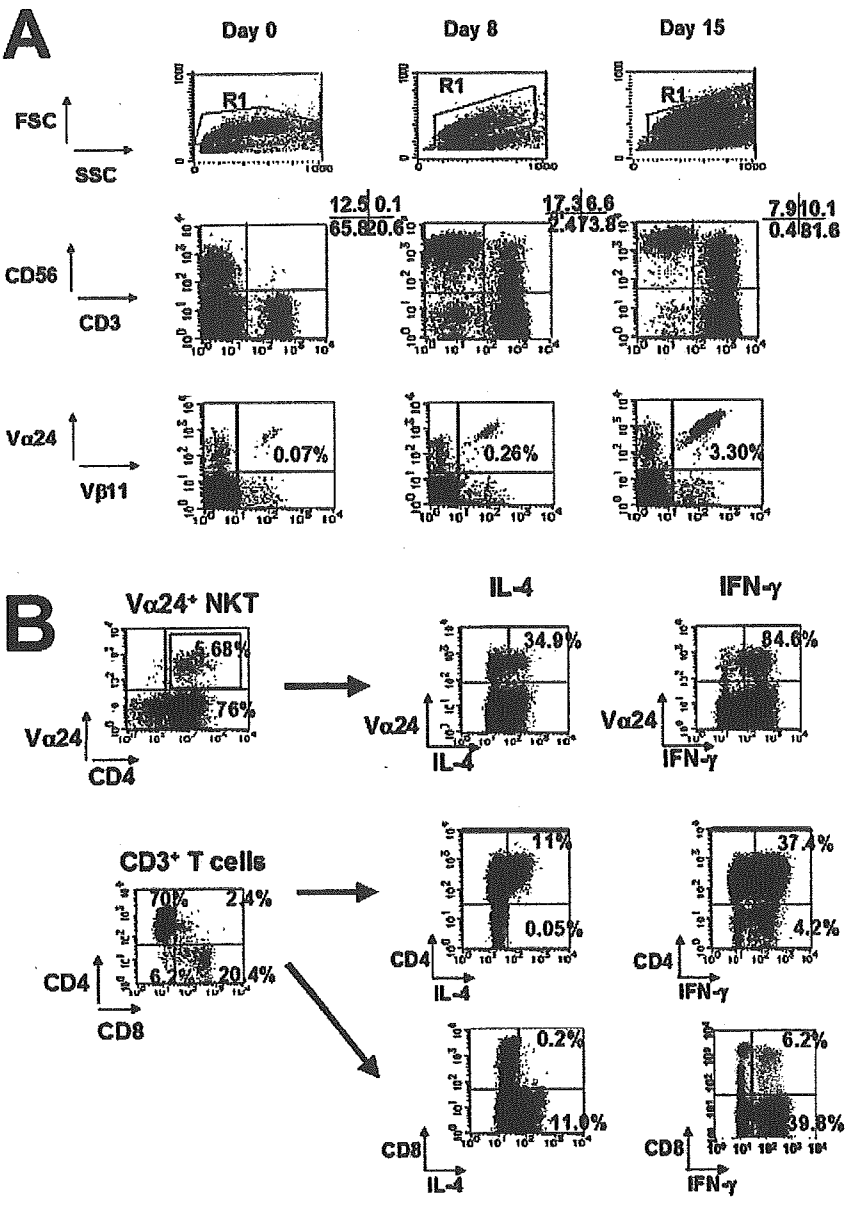

Figure 4. (A) Percentages of T and NK cells (R1 gated; middle part) and Vα24$^+$Vβ11$^+$ NKT cells (CD3$^+$ T cell gated; lower part) at day 0 and after 8 or 15 days of culture with IL-15, IL-7, Flt3-L and αGalCer from day 0. (B) IL-4 and IFN-γ secretion by cultured Vα24$^+$Vβ11$^+$ NKT cells (CD4$^+$ gated) and other T cell compartments. On day 15, the expanded CD4$^+$ single-positive Vα24$^+$Vβ11$^+$ NKT cells produced IL-4 and also IFN-γ (upper part). The remaining post-cultured CD4$^+$ T cells also produced IL-4 and IFN-γ, whereas CD8$^+$ T cells secreted IFN-γ alone (lower part). Control experiment was made without stimulation with PMA and ionomycin.

detected, but CD3$^+$ T cells showed the same phenotype as in the presence of αGalCer (data not shown).

Cytokine secretion profile of expanded Vα24$^+$Vβ11$^+$ NKT cells

Cytokine secretion of expanded Vα24$^+$Vβ11$^+$ NKT cells was investigated by examining the intracellular expression of IFN-γ as Th1 cytokine and of IL-4 as Th2 cytokine. On day 15, the expanded CD4$^+$ single-positive Vα24$^+$Vβ11$^+$ NKT cells produced both IL-4 and IFN-γ (Fig. 4B). CD4$^+$ T cells produced both IL-4 and IFN-γ, while CD8$^+$ T cells secreted IFN-γ only. On the other hand, without expansion of CD4$^+$ Vα24$^+$Vβ11$^+$ NKT cells by αGalCer, the CD4/CD8 ratio and the cytokine secretion of T cells did not change significantly (data not shown).

Cytotoxic activity against K562 cells

We evaluated the effect of Vα24$^+$Vβ11$^+$ NKT cells on the cytotoxic activity of the cultured CBMNC against K562 cells, an erythroleukemic cell line, as described in Materials and methods. Fresh CBMNC showed a

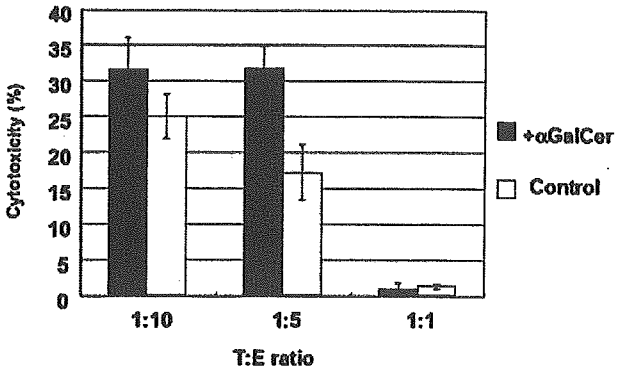

Figure 5. Comparison of the cytotoxic activity of the cultured CBMNC against K562 cells. On day 15, cells cultured in the presence (filled bar) or absence (open bar) of αGalCer were examined for their cytotoxic activity against K562 cells. The effector cells (E) and target cells (T) were mixed to obtain T : E ratios of 1 : 10, 1 : 5 and 1 : 1. One representative of three independent experiments is shown.

minimal cytotoxic activity against K562 cells, while cells cultured for 15 days with αGalCer gained in cytotoxic activity. The CBMNC cultured with αGalCer had an enhanced cytotoxicity against K562 cells compared to the control, but had no significant additive effect on the cytotoxic activity of NK and T cells (p = not significant) (Fig. 5).

Discussion

In the present study, we succeeded in expanding $V\alpha24^+V\beta11^+$ NKT cells from human CBMNC without losing progenitor cells by cell sorting. The expanded $V\alpha24^+V\beta11^+$ NKT cells presented a $CD4^+$ single-positive phenotype and secreted both IL-4 and IFN-γ.

Similarly to mouse $V\alpha14^+V\beta8.2^+$ NKT cells, the activation and proliferation of human $V\alpha24^+V\beta11^+$ NKT cells are CD1d dependent. Previous reports used DC as the strongest antigen-presenting cells for the expansion of $V\alpha24^+V\beta11^+$ NKT cells in adult peripheral blood [18, 19] and in cord blood [20]. However, to avoid the loss of any cell compartments through additional manipulations, we describe here a method to easily expand $V\alpha24^+V\beta11^+$ NKT cells in the presence of IL-15, IL-7 and Flt3-L without DC induction.

Ueda *et al.* succeeded in expanding $V\alpha24^+V\beta11^+$ NKT cells by adding αGalCer directly to fresh CBMNC in the presence of IL-2 [22]. IL-15 has been recently reported as one of the cytokines involved in monocyte differentiation into mature DC, the strongest antigen-presenting cells [34, 35]. In our system, we observed a 2300-fold expansion of $V\alpha24^+V\beta11^+$ NKT cells after 15 days, although DC did neither proliferate nor maturate.

According to the results of our depletion analysis, monocytes constituted the $CD1d^+$ cell compartment critically involved in NKT cell expansion, whereas B cells and DC were not required. $CD4^+$ $V\alpha24^+V\beta11^+$ NKT cells did not proliferate for more than 15 days in the presence of IL-15, IL-7, Flt3-L and αGalCer. This phenomenon seemed to be correlated with the decrease of the CD1d-presenting cells.

The complexity of the NKT cell phenotype in mice was emphasized by several classifications [36]. Using CD1d tetramers loaded with αGalCer, four subsets of NKT cells were identified, differing in NK1.1 expression, TCR repertoire and CD1d-dependence [37, 38]. These different subsets might explain the paradoxical properties of NKT cells, as CD1d-restricted NKT cells inhibited tumor growth in some cases, but could also suppress anti-tumor immunity in other experiments [12, 39]. Although mouse CD1d-αGalCer tetramers stained human NKT cells, further studies are required to characterize human NKT cell specificities. In our system, expanded $V\alpha24^+V\beta11^+$ NKT cells were CD4 single positive and produced both IL-4 and IFN-γ. IL-7 up-regulates IL-4 production by NKT cells in mice [40], but we did not observe any Th2 polarization despite the presence of IL-7 in the culture medium. Lin *et al.* have tested different cytokines to expand NKT cells from peripheral blood mononuclear cells [16]. IL-2 and IL-15 resulted in the best expansion rate, and IL-15 enhanced the cytotoxic activity of NKT cells against U937 cells after 7 days of culture. Both IL-7 and IL-15 preferentially expanded $CD4^-CD8^-$ NKT cells, and the authors proposed to combine those two cytokines for an optimal anti-tumor application of NKT cells. However, in our study, $CD4^+$ NKT cells were predominant when CBMNC were expanded with IL-15, IL-7 and Flt3-L, and they produced both Th1 and Th2 cytokines. Cord blood-derived NKT cells may have specific properties compared to peripheral blood-derived NKT cells.

Whether human $V\alpha24^+V\beta11^+$ NKT cells exhibit direct cytotoxic activity is still controversial [41]. Because $V\alpha24^+V\beta11^+$ NKT cells produce huge amounts of cytokines rapidly after αGalCer stimulation, they may act preferentially by stimulating other effector cells such as NK or CD8 T cells. In our system, the cytotoxicity of CBMNC against K562 cells was enhanced after 15 days of culture. However, the $V\alpha24^+V\beta11^+$ NKT cell expansion did not enhance the cytotoxicity of NK cells. As $CD4^+$ NKT cells produce both Th1 and Th2 cytokines, they may not influence the anti-tumoral response of NK cells. The culture of CBMNC with or without αGalCer did not change T and NK cell compartments either. The CD4/CD8 ratio remained stable, as was the cytokine profile of $CD4^+$ and $CD8^+$ T cells (data not shown).

The role of NK cells in acute GVHD and the GVL effect may be as important as that of T cells [42]. In our

system, the fact that $CD8^+$ T and NK cells increased significantly after 15 days of culture might result in enhancing not only the GVL effect but also GVHD. The effect of activated NK cells and $V\alpha24^+V\beta11^+$ NKT cells on these $CD8^+$ T cells remains to be further investigated.

In conclusion, our method for expanding $V\alpha24^+V\beta11^+$ NKT cells derived from CBMNC is easy to perform and may be helpful for future clinical use.

Materials and methods

Human umbilical cord blood

Human umbilical cord blood samples were obtained during normal full-term deliveries after obtaining informed consent. We used samples that were not processed by the Tokyo Cord Blood Bank for therapeutic use because of the small volume (less than 40 mL) or the time elapsed. Cord blood samples were stored at room temperature and processed within 36 h of collection.

αGalCer

αGalCer (KRN7000) was dissolved in DMSO and used at a concentration of 100 ng/mL for cell culture. Control experiments were done with βGalCer, an analogue of αGalCer. αGalCer and βGalCer were kindly provided by Kirin Brewery Co, Ltd. (Gunma, Japan).

Cytokines

Recombinant human IL-15, IL-7 and Flt3-L were purchased from Peprotech (London, UK) and used for cell culture at the indicated concentrations.

Cell culture

CBMNC were isolated by Ficoll-Paque (Sigma, 87. Louis, USA) density gradient centrifugation and washed twice with PBS. CBMNC (1×10^6 cells/mL) were suspended in complete RPMI 1640 medium supplemented with 10% heat-inactivated FBS, 0.01 mM nonessential amino acids, 1 mM sodium pyruvate, 100 U/mL penicillin, 100 μg/mL streptomycin and 250 ng/mL amphotericin B, and cultured in 6-well plates (2×10^6 cells/well). IL-15 and/or IL-7 and/or Flt3-L were added at the indicated concentrations, and half of the medium was changed every 4–5 days with or without addition of αGalCer. The number of viable mononuclear cells was counted after Trypan blue staining. The absolute number of cells per well was calculated by multiplying the percentage of each subpopulation of CBMNC, measured by FACS analysis, by the total number of viable mononuclear cells.

Flow cytometric analysis

Cell surface markers were analyzed with a FACS Calibur using Cell Quest software (Becton Dickinson, Mountain View, CA). Fresh or cultured cells were suspended in PBS, incubated with mouse serum to block nonspecific binding, and stained for 20 min on ice with specific FITC-, PE- or allophycocyanin-conjugated mouse monoclonal antibodies (mAb). Anti-CD3, -CD19, -CD1a, -CD4, -CD8α and -TCRαβ mAb were purchased from e-Bioscience (CA, USA). Anti-Vα24 (C15) and anti-Vβ11 (C21) mAb were purchased from Coulter-Immunotech (Marseille, France). Anti-CD56, -CD14, -TCRγδ mAb and isotype controls were purchased from BD Pharmingen (CA, USA). PE- and FITC-conjugated anti-IL-4 and anti-IFN-γ antibodies were also from BD Pharmingen and were used for intracellular staining. Dead cells were stained by propidium iodide and gated out. The CBMNC were gated by forward scatter and side scatter, and then $CD3^+$ cells were analyzed. $CD3^+CD4^+CD8^+$ cells were considered as double-positive cells, but doublet formation had not been formally excluded.

AutoMACS depletion assay

Fresh CBMNC were stained with PE-labeled anti-CD14, anti-CD19, and/or anti-CD1a antibodies and were depleted using anti-PE beads in an AutoMACS magnetic sorting system (Miltenyi Biotec GmbH, Germany). Monocytes, B cells, DC or all of these three antigen-presenting cells were depleted, and the remaining cells were cultured with 50 ng/mL IL-15, 10 ng/mL IL-7, 10 ng/mL Flt3-L and 100 ng/mL αGalCer for 15 days as described above.

Intracellular staining

To detect intracellular expression of IL-4 and IFN-γ, cultured CBMNC were stimulated with 1 ng/mL PMA (Sigma, St. Louis, MO) and 2 μM ionomycin (Sigma) in the presence of 2 μM monensin (Sigma) for 4 h. Cells were then washed twice with PBS containing 0.5% BSA and 0.1% sodium azide (PBS/BSA/Azide) and stained for surface markers using fluorescence-conjugated mAb and ethidium monoazide bromide. Cells were fixed in 4% paraformaldehyde (Wako, Japan) for 20 min at room temperature, washed and permeabilized with PBS/BSA/Azide with 0.5% saponin for 10 min. Cells were then incubated with the anti-IL-4 or IFN-γ mAb for 30 min, washed twice and analyzed in a FACS Calibur.

Cytotoxic assay

Analysis of cytotoxic activity against K562 cells was performed with pre-cultured and post-cultured CBMNC using a non-radioactive cytotoxic assay, CytoTox 96 (LDH release methods; Promega, USA). The effector cells (E) and target cells (T) were mixed to obtain T : E ratios of 1 : 10, 1 : 5 and 1 : 1, and incubated for 4 h in 100 μL phenol red-free RPMI 1640 supplemented with 5% FBS in 96-well plates. Target cells were plated at 2×10^4 cells/well. Analysis and calculation were described elsewhere [27].

Statistics

Results are reported as means ± SD from more than three experiments. Significance levels were determined by analysis of variance (ANOVA) followed by the Dunett post-test for differences in means, using JMP software (SAS Institute Inc.).